



HAL
open science

Metabolic Cooperation among Commensal Bacteria Supports *Drosophila* Juvenile Growth under Nutritional Stress

Jessika Consuegra, Théodore Grenier, Houssam Akherraz, Isabelle Rahioui, Hugo Gervais, Pedro da Silva, François Leulier

► **To cite this version:**

Jessika Consuegra, Théodore Grenier, Houssam Akherraz, Isabelle Rahioui, Hugo Gervais, et al.. Metabolic Cooperation among Commensal Bacteria Supports *Drosophila* Juvenile Growth under Nutritional Stress. *iScience*, 2020, 23 (6), pp.101232. 10.1016/j.isci.2020.101232 . hal-02998964

HAL Id: hal-02998964

<https://hal.science/hal-02998964>

Submitted on 12 Nov 2020

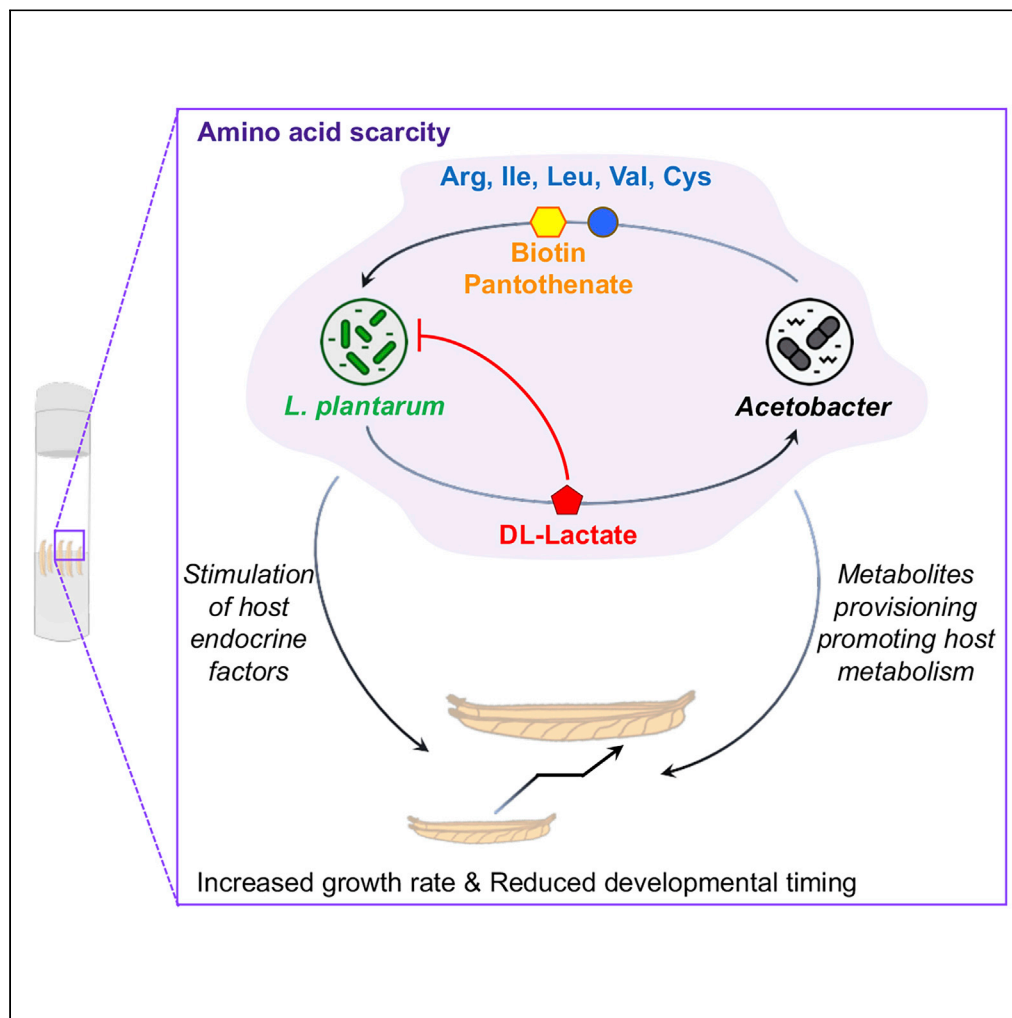
HAL is a multi-disciplinary open access archive for the deposit and dissemination of scientific research documents, whether they are published or not. The documents may come from teaching and research institutions in France or abroad, or from public or private research centers.

L'archive ouverte pluridisciplinaire **HAL**, est destinée au dépôt et à la diffusion de documents scientifiques de niveau recherche, publiés ou non, émanant des établissements d'enseignement et de recherche français ou étrangers, des laboratoires publics ou privés.



Distributed under a Creative Commons Attribution 4.0 International License

Article

Metabolic Cooperation among Commensal Bacteria Supports *Drosophila* Juvenile Growth under Nutritional Stress

Jessika Consuegra, Théodore Grenier, Houssam Akherraz, Isabelle Rahioui, Hugo Gervais, Pedro da Silva, François Leulier

jessika.consuegra@ens-lyon.fr (J.C.)
francois.leulier@ens-lyon.fr (F.L.)

HIGHLIGHTS

L. plantarum feeds lactate to *A. pomorum*

A. pomorum supplies essential amino acids and vitamins to *L. plantarum*

Microbiota metabolic dialogue boosts *Drosophila*'s larval growth

Lactate utilization by *Acetobacter* releases anabolic metabolites to larvae

Consuegra et al., iScience 23, 101232
June 26, 2020 © 2020 The Authors.
<https://doi.org/10.1016/j.isci.2020.101232>

Article

Metabolic Cooperation among Commensal Bacteria Supports *Drosophila* Juvenile Growth under Nutritional Stress

Jessika Consuegra,^{1,*} Théodore Grenier,¹ Houssam Akherraz,¹ Isabelle Rahioui,² Hugo Gervais,¹ Pedro da Silva,² and François Leulier^{1,3,*}

SUMMARY

The gut microbiota shapes animal growth trajectory in stressful nutritional environments, but the molecular mechanisms behind such physiological benefits remain poorly understood. The gut microbiota is mostly composed of bacteria, which construct metabolic networks among themselves and with the host. Until now, how the metabolic activities of the microbiota contribute to host juvenile growth remains unknown. Here, using *Drosophila* as a host model, we report that two of its major bacterial partners, *Lactobacillus plantarum* and *Acetobacter pomorum*, engage in a beneficial metabolic dialogue that boosts host juvenile growth despite nutritional stress. We pinpoint that lactate, produced by *L. plantarum*, is utilized by *A. pomorum* as an additional carbon source, and *A. pomorum* provides essential amino acids and vitamins to *L. plantarum*. Such bacterial cross-feeding provisions a set of anabolic metabolites to the host, which may foster host systemic growth despite poor nutrition.

INTRODUCTION

In the animal kingdom, juvenile growth takes place during the post-natal stages preceding sexual maturation and ushers in the most profound physiological changes in an organism's lifetime. These changes are governed by the complex interplay between the animal's genotype and its nutritional environment. In humans, chronic undernutrition at the juvenile stage leads to severe stunting and long-term negative neurological, metabolic, and reproductive consequences (Goyal et al., 2015). Today 155 million children are plagued by childhood malnutrition worldwide (Development Initiatives, 2018).

Recent studies establish that the microbial communities colonizing the body surfaces (i.e., microbiota), especially the activities and constituents of the gut microbiota, can alter the host's growth trajectory. Both in invertebrates and in mammals, selected strains of microbiota members can buffer the deleterious impact of undernutrition on juvenile growth dynamics (Blanton et al., 2016; Schwarzer et al., 2016; Shin et al., 2011; Smith et al., 2013; Storelli et al., 2011). In humans, children suffering from malnutrition carry an "immature" gut microbiota that fails to be remedied by classical re-nutrition strategies (Subramanian et al., 2014).

Juvenile growth is marked by the exponential increase of the animals' biomass manifested as gain in weight and longitudinal size. These physical traits are governed by the host's growth hormone and growth factors (GH/IGF1 in mammals) whose production and activities are regulated by nutrients availability (Thissen et al., 1994). Recently, it was established that gut microbiota members also influence the production and activity of growth hormone and growth factors in both invertebrate and mammals (Schwarzer et al., 2016; Shin et al., 2011; Storelli et al., 2011; Yan et al., 2016).

Despite recent progress, how the gut microbiota confers such benefits to the host remains poorly understood. This is partly due to the fact that the gut microbiota is a complex ecosystem comprising up to hundreds of microbial species in mammals, mostly bacteria (Hooper and Gordon, 2018). They construct multiplex, high-order nutritional and metabolic networks among themselves and with the host such that these interactions directly influence host nutrition and metabolism (Schroeder and Bäckhed, 2016). Given

¹Institut de Génomique Fonctionnelle de Lyon, Université de Lyon, Ecole Normale Supérieure de Lyon, Centre National de la Recherche Scientifique, Université Claude Bernard Lyon 1, UMR5242, 69364 Cedex 07, Lyon, France

²Laboratoire Biologie Fonctionnelle, Insectes et Interactions, Université de Lyon, Institut National des Sciences Appliquées, Institut National de Recherche pour l'Agriculture, l'Alimentation et l'Environnement, UMR0203, 69621 Villeurbanne, France

³Lead Contact

*Correspondence: jessika.consuegra@ens-lyon.fr (J.C.), francois.leulier@ens-lyon.fr (F.L.)

<https://doi.org/10.1016/j.isci.2020.101232>



this complexity, until now no study has elucidated to what extent and how the metabolic interactions among members of the microbiota contribute to host juvenile growth.

To answer this question, we bypassed the complexity encountered in mammals and developed an experimentally tractable gnotobiotic *Drosophila* model associated with its two major bacterial partners, *Lactobacillus plantarum* and *Acetobacter pomorum*, which are frequently found to co-exist in wild flies captured on fruit-based baits (Chandler et al., 2011; Pais et al., 2018; Wong et al., 2013). Previously, using oligidic diets (i.e., a diet composed of complex ingredients such as inactivated yeast and cornmeal flour), we and others have established that association of germ-free (GF) larvae with either *A. pomorum* or *L. plantarum* stimulates juvenile growth by promoting the systemic release and activities of *Drosophila* insulin-like peptides (dILPs), the functional analogs of vertebrate insulin and IGFs (Shin et al., 2011; Storelli et al., 2011). Here, using *Drosophila* bi-associated with *A. pomorum* and *L. plantarum*, we characterized the metabolic dialogues among the three partners in a strictly controlled nutritional environment low in amino acids to mimic chronic protein undernutrition, namely, a fully chemically defined or holidic diet (HD) (Piper et al., 2017). HDs support suboptimal growth and development of *Drosophila* larvae (Jang and Lee, 2018; Piper et al., 2013; Rapport et al., 1983; Schultz et al., 1946), yet it has proved to be a useful tool to study the specific influence of individual nutrients on *Drosophila* physiology (Jang and Lee, 2018; Mishra et al., 2018; Piper et al., 2013, 2017). This experimental model grants us complete control over three key parameters in the system: the diet, the host, and its commensal partners. We defined the nutritional requirements, auxotrophies, and complementation of over 40 individual nutrients including all amino acids, vitamins, nucleic acids, lipid precursors, and minerals for each commensal and the juvenile host in the GF context or upon association with either microbial partner (Consuegra et al., 2020).

Here, we report that, when co-inoculated on a *Drosophila* HD low in amino acids, *L. plantarum* and *A. pomorum* engage in a beneficial metabolic dialogue that supports bacterial growth and buffers the deleterious impact of nutritional stress on host juvenile growth. We specifically pinpoint that lactate, the main metabolic by-product of *L. plantarum*, is utilized by *A. pomorum* as an additional carbon source, and in turn, *A. pomorum* provides various amino acids and B vitamins to complement *L. plantarum* auxotrophies. Inert microbial biomass has been reported to promote larval development (Bing et al., 2018; Storelli et al., 2011) and adult longevity (Keebaugh et al., 2018; Yamada et al., 2015) probably by acting as an additional nutritional source. Although we confirm that inert bacterial biomass slightly contributes to increased juvenile growth, we show that *Lactobacillus* provision of lactate to *Acetobacter* triggers a metabolic shift in *Acetobacter* leading to the provision of a set of anabolic metabolites to the host, which may boost host systemic growth despite poor nutrition.

RESULTS

Bi-Association Enhances the Benefit of Commensal Bacteria on Larval Development

In a Holidic Diet (HD) low in amino acids that mimics chronic protein undernutrition, we studied larval development in germ-free (GF) and upon mono or bi-association with two representative commensal strains of the *Drosophila* microbiota: *Acetobacter pomorum*^{WJL} (Ap^{WJL}) and *Lactobacillus plantarum*^{NC8} (Lp^{NC8}). In this diet, GF larvae reach metamorphosis at ~10 days. By comparison, the time from embryogenesis to metamorphosis of GF animals on rich oligidic diets (i.e., yeast, 50 g/L) is ~5 days, whereas it is increased to ~13 days on poor oligidic diet (i.e., yeast, 6 g/L) (Matos et al., 2017).

On HD, the benefit on larval development of bacterial mono-association is enhanced in larvae bi-associated with Ap^{WJL} and Lp^{NC8} (Ap^{WJL}:Lp^{NC8}; Figures 1A and 1B). Bi-associated animals always develop faster than their mono-associated siblings and reach metamorphosis in ~5.2 days (Figure 1A) or ~8.2 days (Figure 1B) according to the initial bacterial inoculum. We observed similar results using both complete HDs with optimal amino acid content (Figure S1A, HD 16 g and HD 20 g) or with a fruit-based diet (banana diet, Figure S1B) containing ~7 g/kg of protein (Oyeyinka and Afolayan, 2019) where GF larvae fail to develop (see Methods). Of note, the differential capacities of the bacteria to sustain *Drosophila* growth on the banana diet are not a consequence of differential bacteria growth on this fruit-based diet as both Ap^{WJL} and Lp^{NC8} grew to the same extent in the presence or absence of larvae (Figures S1C and S1D).

During post-embryonic development, Ap^{WJL} or Lp^{NC8} not only influences maturation rates (i.e., time to entry to metamorphosis) but also increases larval linear size gains upon nutrient scarcity (Figure 1C).

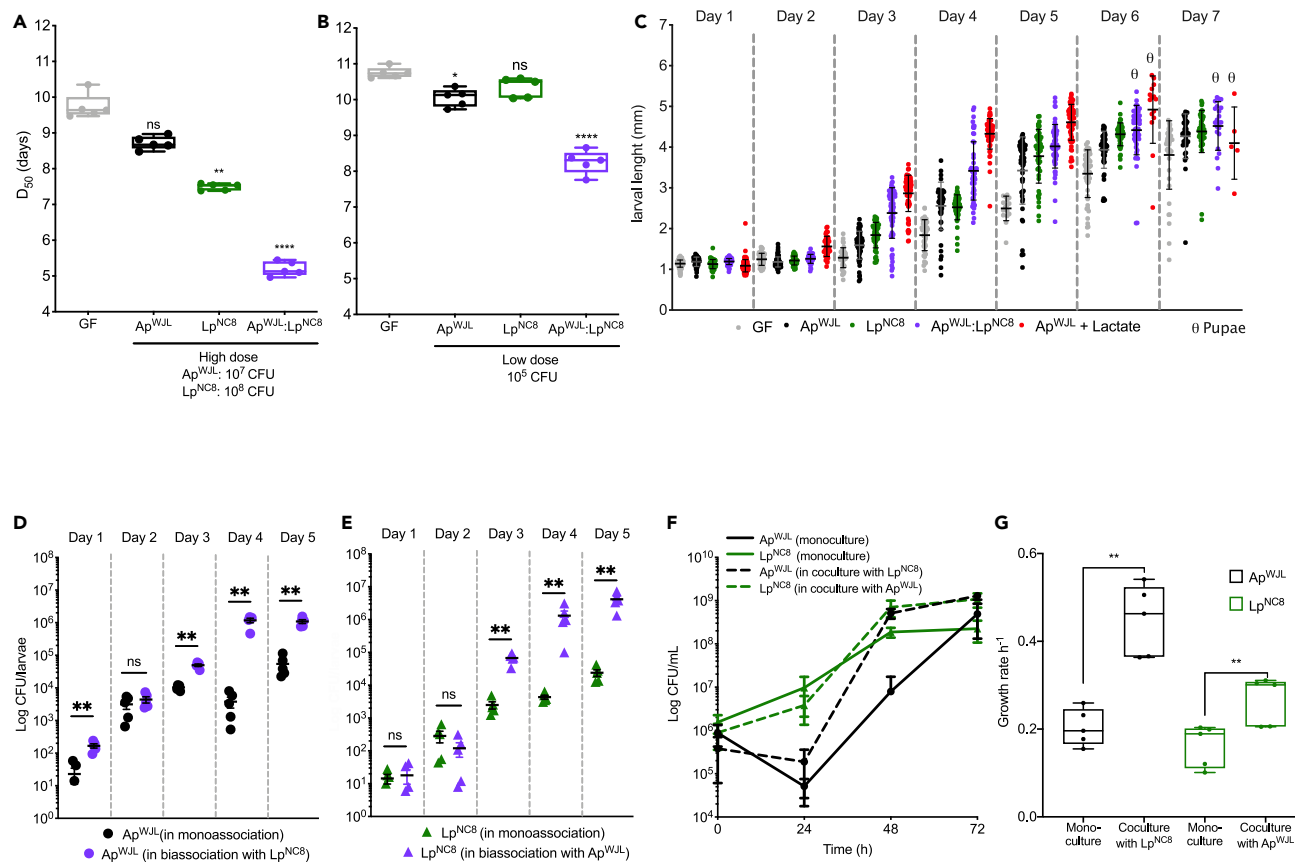


Figure 1. Bi-Association with Ap^{WJL} and Lp^{NC8} Enhances Commensal-Mediated Benefit on Larval Development

(A and B) Developmental timing (time from egg to metamorphosis) on complete holidic diet (HD) of Germ-Free (GF) larvae (gray) or GF larvae inoculated with high dose (10^7 or 10^8 CFU) respectively; (A) or low dose (10^5 CFU); (B) of Ap^{WJL} and/or Lp^{NC8} (Ap^{WJL} , black; Lp^{NC8} , green; $Ap^{WJL}:Lp^{NC8}$, purple). D_{50} : Day when 50% of the larvae population has entered metamorphosis.

(C) Larval length at every day post-embryogenesis of GF larvae or post-inoculation (Day 1) with 10^5 CFU of Ap^{WJL} and/or Lp^{NC8} or Ap^{WJL} mono-associated larvae supplemented with DL-lactate at a final concentration of 0.6 g/L (red). θ , pupae detected in the vial.

(D and E) Microbial load (Ap^{WJL} , D; Lp^{NC8} , E) of larvae mono- or bi-associated with 10^5 CFU of Ap^{WJL} and/or Lp^{NC8} .

(F and G) Growth in liquid HD (F) and growth rates (G) of Ap^{WJL} and Lp^{NC8} in mono- (plain lines) or cocultures (dashed lines) in liquid HD. Gray always refers to GF, black to Ap^{WJL} mono-association, green to Lp^{NC8} mono-association condition, and purple to $Ap^{WJL}:Lp^{NC8}$ bi-association. Each symbol represents an independent replicate except in (F) where symbols represent the means \pm SEM of three biological replicates. Boxplots show minimum, maximum, and median where each point is a biological replicate. Dot plots show mean \pm SEM. (A and B) We performed Kruskal-Wallis test followed by uncorrected Dunn's tests to compare each gnotobiotic condition with GF. (D and E) Each point represents a biological replicate comprising the average microbial load of a pool of 10 larvae. We performed Mann-Whitney test to compare microbial loads in mono-association with microbial loads in bi-association for the strain of interest at each time point. (G) We performed Mann-Whitney test to compare the growth rate in monoculture to the growth rate in coculture for the strain of interest.

ns: non-significant, *: p value < 0.05, **: p value < 0.005, ***: p value < 0.0005, ****: p value < 0.0001. See also Figures S1 and S2.

$Ap^{WJL}:Lp^{NC8}$ bi-association also enhances the benefit of commensals on this trait as early as 3 days after bi-association (Figure 1C).

Next, we wondered if each bacterium benefits from the presence of the other. To this end, we assessed the microbial load in larvae through larval development upon mono- and bi-association with Ap^{WJL} , Lp^{NC8} or $Ap^{WJL}:Lp^{NC8}$, respectively. Ap^{WJL} and Lp^{NC8} loads in mono- or bi-association start to differ from day 3 after egg laying and reach a two-log difference at day 5 (Figures 1D and 1E). The reciprocal benefit between Ap^{WJL} and Lp^{NC8} is also observed while bacteria grow in a liquid version of the HD (see Methods). In coculture, Ap^{WJL} and Lp^{NC8} have slightly higher final biomasses (Figure 1F) and marked higher growth rates (Figure 1G) than in mono-cultures. As previously reported in other experimental settings, the enhanced benefit of commensals on fly's lifespan (Yamada et al., 2015) or larval development (Bing et al., 2018; Storelli et al., 2011) is mediated at least partly by the trophic effect of providing inert microbial biomass as nutrients to the

host. Since we detected a slightly increased bacterial biomass in the diet and the host upon bi-association, we investigated the contribution of such inert biomass to the observed growth promotion phenotype. To this end, we inoculated GF larvae with Heat Killed (HK) Ap^{WJL} or Lp^{NC8} at high dose (10^9 CFU) in mono- and bi-associated conditions (Figure S2A). Mono-association with HK bacteria at high or low doses fails to accelerate larval development (Figures S2A and S2B), yet bi-association with HK bacteria at high doses slightly contribute to host development by accelerating larval development by ~ 1 day compared with GF animals (Figure S2A). However, this effect is very mild when compared with the effect of live and metabolically active bacteria bi-association at high or low doses (Figures 1A and 1B), which, respectively, led to larval development accelerations of ~ 5.5 or ~ 2.5 days compared with GF conditions. Of note, in contrast to live bacteria bi-association, bi-association with HK bacteria on HDs with an increased amino acid content or a banana diet did not rescue or accelerate larval development (Figures S1A and S1B). Moreover, the enhanced *Drosophila* growth observed upon bi-association requires both bacteria to be metabolically active and associated to the host from early stages of development, since bi-association where one of the bacteria is HK (Figure S2B) or delayed bi-association (Figures S2C and S2D) fails to accelerate larvae development.

Collectively, our results show that microbial bi-association of larvae developing in a suboptimal nutritional context results in increased host's maturation rates and size gains compared with mono-associations. This beneficial effect partially results from a trophic effect of increased bacterial biomass provision to the host but mostly relies on the functional impact of alive and metabolically active microbes.

Ap^{WJL} Benefits Lp^{NC8} via Essential Amino Acid and Vitamins Provision

Recently, we showed that Ap^{WJL} and Lp^{NC8} differentially fulfil the nutritional requirements of the ex-GF larva thanks to their individual genetic repertoires. In this context, the positive impact of Ap^{WJL} or Lp^{NC8} on host development requires metabolically active bacteria and is independent of bacterial loads in the depleted diets or in the larval gut (Consuegra et al., 2020). Specifically, we identified the nutritional auxotrophies of both Ap^{WJL} and Lp^{NC8} in HD. Ap^{WJL} is completely prototroph, whereas Lp^{NC8} is auxotroph for Arg, Ile, Leu, Val, Cys, biotin, and pantothenate. Such differences between Ap^{WJL} and Lp^{NC8} were expected. Indeed, *L. plantarum* is a fastidious bacterium with complex metabolic requirements including amino acids and vitamins (Martino et al., 2016; Vos et al., 2009). Therefore, in a simple microbial community like the one studied here, a prototrophic bacterium like *A. pomorum* may support *L. plantarum* growth by providing essential amino acids and vitamins.

To directly test this hypothesis, we studied the growth of Lp^{NC8} in the presence of Ap^{WJL} in liquid HD lacking each of the amino acids and vitamins for which it is auxotroph. We set monocultures of Ap^{WJL} and Lp^{NC8} and a coculture of $Ap^{WJL}:Lp^{NC8}$ in liquid HD Δ Arg, Δ Ile, Δ Leu, Δ Val, Δ Cys, Δ Biotin, or Δ Pantothenate and assessed the bacterial counts in mono and cocultures during 72 h. As expected, Ap^{WJL} grows in these media to the same extent as in the complete HD, whereas Lp^{NC8} is unable to grow as a monoculture (Figures 2A–2G). Interestingly, Lp^{NC8} grows in the deficient media only when cocultured with Ap^{WJL} (Figures 2A–2G). From the HD Δ Arg, HD Δ Ile, and HD Δ Leu mono- and cocultures, we also recovered supernatants and quantified Arg, Ile, and Leu release in the media using high-performance liquid chromatography (HPLC). In Ap^{WJL} monocultures, we observe an accumulation of these amino acids that correlates with Ap^{WJL} growth (Figures 2H–2J). As expected, they are not detected in the Lp^{NC8} monocultures (Figures 2H–2J). In $Ap^{WJL}:Lp^{NC8}$ coculture, we do not detect any accumulation of Arg or Leu and a reduction in Ile accumulation, which suggests that the amino acids released by Ap^{WJL} are immediately consumed by Lp^{NC8} to support its growth and thus do not accumulate in the media (Figures 2H–2J). These results therefore establish that Ap^{WJL} provides amino acids, and probably B vitamins to Lp^{NC8} .

Ap^{WJL} to Lp^{NC8} Nutrient Provision Potentiates Commensal-Mediated Larval Auxotrophies Compensation

Next, we sought to determine if these metabolic interactions among *Drosophila* commensals could be translated into a further benefit to larvae developing on media lacking each of the amino acids and vitamins for which Lp^{NC8} is auxotrophic. We therefore assessed the developmental time in HD Δ Arg, Δ Ile, Δ Leu, Δ Val, Δ Cys, Δ Biotin, and Δ Pantothenate of mono- (Ap^{WJL} or Lp^{NC8}) or bi-associated ($Ap^{WJL}:Lp^{NC8}$) larvae (Figure 2K). Association of the larval host with Ap^{WJL} compensates all nutrient depletions except for pantothenate, whereas Lp^{NC8} fails to compensate the lack of any nutrient for the host because of its own

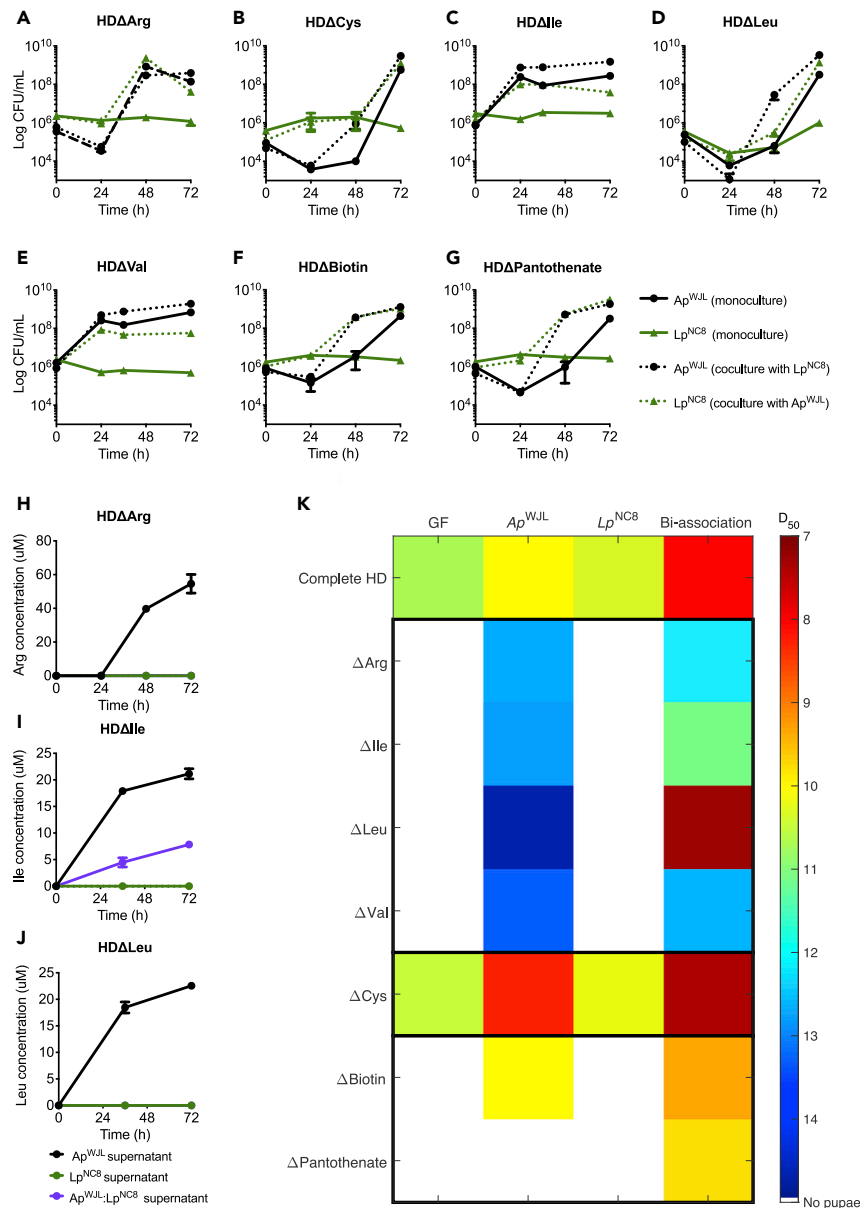


Figure 2. *Ap*^{WJL} Benefits *Lp*^{NC8} via Essential Amino Acid and Vitamins Provision

(A–G) Growth curves of *Ap*^{WJL} and *Lp*^{NC8} in mono- (plain lines) or cocultures (dotted lines) in liquid holidic diets (HD) lacking Arg (HDΔArg) (A), Cys (HDΔCys) (B), Ile (HDΔIle) (C), Leu (HDΔLeu) (D), Val (HDΔVal) (E), Biotin (HDΔBiotin) (F) or Pantothenate (HDΔPantothenate) (G). Black refers to *Ap*^{WJL}, green the *Lp*^{NC8}.

(H–J) HPLC quantification of Arg, Ile, and Leu in *Ap*^{WJL} or *Lp*^{NC8} mono-culture supernatants (black and green lines, respectively) or *Ap*^{WJL}:*Lp*^{NC8} coculture (purple line) in HDΔArg, HDΔIle, HDΔLeu, respectively. (A–J) Symbols represent the means ± SEM of three biological replicates.

(K) Heatmap representing the mean *D*₅₀ (day when 50% of the larvae population has entered metamorphosis) of GF larvae (first column) and larvae mono-associated with *Ap*^{WJL} or *Lp*^{NC8} or bi-associated with *Ap*^{WJL}:*Lp*^{NC8} (columns 2, 3, and 4, respectively). Each row shows *D*₅₀ in a different version of the HD: complete HD or HDs each lacking a specific nutrient HDΔArg, HDΔIle, HDΔLeu, HDΔVal, HDΔCys, HDΔBiotin, HDΔPantothenate. White color code means that larvae did not reach pupariation.

auxotrophies. Interestingly, bi-association with *Ap*^{WJL}:*Lp*^{NC8} systematically exceeds the benefit provided to the host by mono-association with *Ap*^{WJL}, and in HDΔPantothenate even rescues host viability (Figure 2K).

Taken together, these results establish that upon bi-association, Ap^{WJL} supplies Arg, Ile, Leu, Val, Cys, biotin, and pantothenate to Lp^{NC8}, thus allowing both commensals to thrive on these depleted media. This nutritional cooperation then potentiates the commensal-mediated promotion of larval development in depleted diets via the bacterial provision of the missing essential nutrients to the host.

Lp^{NC8}-Derived Lactate Benefits Ap^{WJL} and Enhances Ap^{WJL}-Mediated Larval Growth Promotion

Next, we wondered how Ap^{WJL} benefits from Lp^{NC8} (Figures 1F and 1G). We hypothesize that Lp^{NC8} metabolic by-products enhance the ability of Ap^{WJL} to promote larval development. To test this, we mono-associated GF embryos with Ap^{WJL} and added either sterile PBS or the supernatant of a culture of Lp^{NC8} grown on liquid HD for 3 days. The addition of an Lp^{NC8} supernatant on embryos mono-associated with Ap^{WJL} is sufficient to accelerate larval development by ~4 days compared with GF animals, whereas Ap^{WJL} mono-association only triggers a single day acceleration. However, addition of Lp^{NC8} supernatant did not improve larval development in GF condition or in mono-association with Lp^{NC8} (Figure 3A).

L. plantarum is a homolactic fermentative microorganism that secretes its principal metabolic by-products D- and L-lactate into the nutritional substrate. We next assayed if an equimolar solution of DL-lactate could reproduce the benefit of Lp^{NC8} supernatant on embryos mono-associated with Ap^{WJL}. When DL-lactate is added at a final concentration of 0.6 g/L, larvae mono-associated with Ap^{WJL} exhibit strong developmental acceleration and linear size gain (Figures 3B and 1C). However, DL-lactate is deleterious to GF larvae as it delays development by ~2 days (Figure 3B). Furthermore, in HD lacking each of the fly essential amino acids (Figure 3C) or in complete HDs with optimal amino acid content (Figure S1A, HD 16g and HD 20g), the DL-lactate supplementation to larvae mono-associated with Ap^{WJL} reproduces and even exceeds the benefit of the bi-association.

A. pomorum is an acetic acid bacterium that produces acetic acid by aerobic fermentation. We first confirmed that Ap^{WJL} does not produce lactate during growth on liquid HD (Figure 3D) but is capable of consuming exogenous sources of lactate in the cultured media, without a preference of either chiral form (Figure 3E). Consumption of DL-lactate by Ap^{WJL} slightly increases its final biomass in solid HD (Figures S3A and S3B), reaching an average ~4x10⁷ CFU/tube (instead of ~1x10⁷ CFU/tube when lactate was omitted) and markedly enhances bacterial growth rate in both liquid (Figure 3F) and solid HD with or without larvae (Figures 3G, 3H, S3A, and S3B). In liquid HD, we quantified that Lp^{NC8} releases ~8 g/L of DL-lactate (3:1 ratio, D:L; Figure 3I). Finally, in an Ap^{WJL}:Lp^{NC8} coculture, we observed that the lactate released by Lp^{NC8} is immediately consumed by Ap^{WJL}, preventing its accumulation in the media (Figure 3J).

Next, we wondered if the beneficial effect on larval development we observed upon supplementation with DL-lactate of Ap^{WJL} mono-associated larvae is due to the mere increase of Ap^{WJL} biomass. To test this hypothesis, we assessed the development of larvae mono-associated with Ap^{WJL} in two conditions: first, with a high dose of Ap^{WJL} biomass (~10⁸ CFU) so it matches the final bacterial count at stationary phase in solid HD supplemented with lactate in the presence of larvae. Second, live Ap^{WJL} biomass associated to *Drosophila* larvae was corrected daily to match the biomass reached when Ap^{WJL} mono-associated animals are supplemented with lactate, according to the bacterial growth dynamics established in Figures S3B–S3D. Mono-association with a higher dose of Ap^{WJL} (10⁸ CFU) was deleterious to larval development (Figure S3D); this also justifies our choice of 10⁷ CFU Ap^{WJL} inoculum in Figure 1A. Indeed, in two of five replicates, flies did not reach pupariation (egg-to-pupae survival <20%, Figure S3E). In the other three replicates, egg-to-pupae survival was higher (~80%) as well as variability among replicates (coefficient of variation [CV] = 17.4%). In the Ap^{WJL} lactate-matched biomass condition, larval development was not faster than larvae mono-associated with Ap^{WJL}, yet lactate supplementation triggered the expected enhanced larval development of Ap^{WJL} mono-associated animals (Figure S3D). Thus, we conclude that the enhanced host growth observed upon lactate supplementation to Ap^{WJL} is not due to the mere increase in Ap^{WJL} biomass and growth rate upon lactate consumption.

The lactate produced by Lp^{NC8} seems to be the key metabolite altering Ap^{WJL} metabolism and its influence on host growth. To directly test this hypothesis, we recovered supernatants of 3-day cultures in liquid HD of an *L. plantarum* strain lacking the *ldh* genes (Lp^{WCF51}Δ*ldhDL*) and its wild-type counterpart (Lp^{WCF51}) and assessed their effects on the development of larvae mono-associated with Ap^{WJL}. Lp^{WCF51}Δ*ldhDL* has

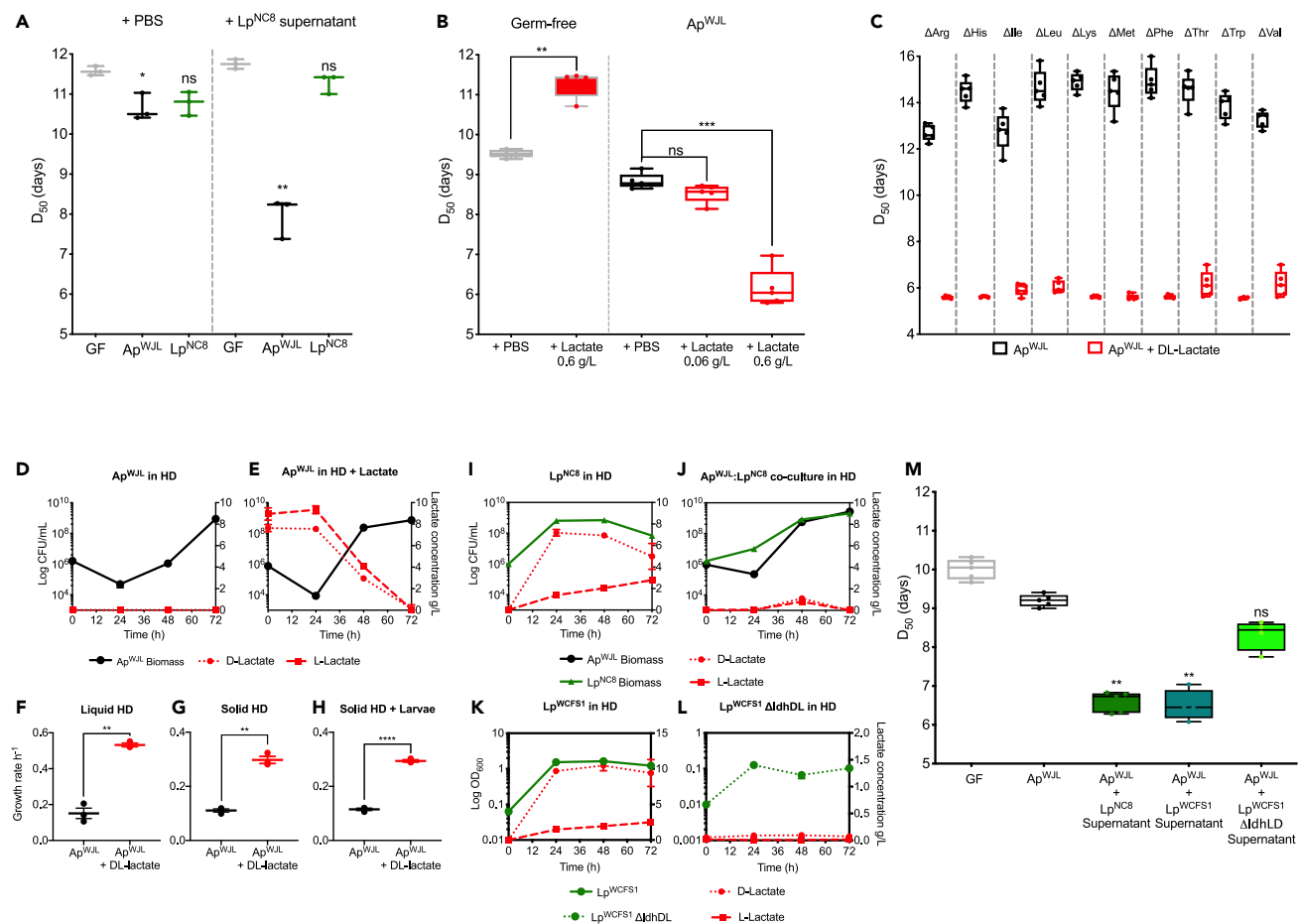


Figure 3. *Lp^{NC8}*-Derived Lactate Benefits *Ap^{WJL}* and Enhances *Ap^{WJL}*-Mediated Larval Growth Promotion

(A and M) Developmental timing of Germ-Free (GF) larvae or GF larvae inoculated with 10^5 CFU of *Ap^{WJL}* (A, M black) or *Lp^{NC8}* (A, green) supplemented with either sterile PBS (A) or the supernatant from a 72-h culture of *Lp^{NC8}* (A, M), *Lp^{WCF51}* (M, turquoise), or *Lp^{WCF51}ΔdhDL* (M, light green) in complete holidic diet (HD).

(B) Developmental timing on HD of GF larvae (gray) or GF larvae inoculated with 10^5 CFU of *Ap^{WJL}* supplemented with either sterile PBS (black) or DL-lactate solutions (red) at inoculation (final concentration in the diet 0.06 or 0.6 g/L). (A, B, and M) Each dot represents an independent biological replicate. Boxplots show minimum, maximum, and median. We performed Kruskal-Wallis test followed by uncorrected Dunn's tests to compare each condition with GF. ns: non-significant, *: p value < 0.05, **: p value < 0.005, ***: p value < 0.0005.

(C–H) (C) Developmental timing of GF larvae inoculated with 10^5 CFU of *Ap^{WJL}* supplemented at inoculation with either sterile PBS (black) or DL-lactate at final concentration of 0.6 g/L in HDs lacking each an essential amino acid for *Drosophila*: from left to right, HDΔArg, HDΔHis, HDΔIle, HDΔLeu, HDΔLys, HDΔMet, HDΔPhe, HDΔThr, and HDΔVal. Boxplots show minimum, maximum, and median, and each dot represents an independent biological replicate. Growth curves (D and E) and growth rates (F) of *Ap^{WJL}* in liquid HD supplemented (E) or not (D) with DL-lactate solution. D- (dotted line) and L-lactate (dashed line) levels (red) were quantified in both conditions. Growth rates of *Ap^{WJL}* in solid HD and HD + DL-lactate with (H) or without (G) larvae.

(I–L) Growth curves in liquid HD of *Lp^{NC8}* (green) or *Ap^{WJL}* (black) in mono- (I) or coculture (J), or *Lp^{WCF51}* (K, green) or *Lp^{WCF51}ΔdhDL* (L, dotted green) with the respective D- (dotted line) or L-lactate (dashed line) levels (red). Note the low OD_{600} of *Lp^{WCF51}ΔdhDL* versus *Lp^{WCF51}* but similar CFU counts (Figures S4A and S4B). Symbols represent the means \pm SEM of three biological replicates except for (F)–(H) where each symbol represents an independent replicate \pm SEM.

See also Figures S1, S3, and S4.

been reported to produce only trace amounts of D- and L-lactate (Ferain et al., 1996). We confirmed these findings in liquid HD by monitoring bacterial growth and DL-lactate production by both strains for 72 h (Figures 3K and 3L). Both strains grow in MRS and liquid HD to the same extent without any difference in their final biomass (CFU/mL) despite the observed reduced OD_{600} of *Lp^{WCF51}ΔdhDL* (Figures S4A and S4B). *Lp^{WCF51}* supernatant at 72 h contains ~ 9.4 g/L of D-lactate and ~ 2.5 g/L of L-lactate (Figure 3K). *Lp^{WCF51}ΔdhDL*, on the other hand, only accumulates a total of ~ 0.09 g/L of DL-lactate (Figure 3L). Importantly, as in an HD + DL-lactate, *Ap^{WJL}* growth rate is higher when growing on *Lp^{NC8}* or *Lp^{WCF51}* supernatants but not on *Lp^{WCF51}ΔdhDL* supernatant (Figure S4C). Also, lactate or lactate-containing supernatants

from Lp^{NC8} or Lp^{WCFS1} sustain increased Ap^{WJL} larval loads during development (Figure S4D), as does bi-association with Lp^{NC8} (Figure 1D). Finally, the addition of a supernatant from Lp^{WCFS1} culture on larvae mono-associated with Ap^{WJL} boosts larval growth and maturation to a degree comparable with Lp^{NC8} 's supernatant (Figure 3M). The effect of these supernatants on host development is not due to secreted bacterial peptides since the total amino acid concentration of Lp^{NC8} culture supernatants remains stable during growth on liquid HD (Figure S4E) and the addition of an equal volume of sterile liquid HD (containing an amount of amino acids similar to the culture supernatant) on larvae mono-associated with Ap^{WJL} does not accelerate development (Figure S4F). Instead, the impact of the tested supernatants on larval development is most likely due to the lactate produced by Lp^{NC8} and Lp^{WCFS1} (Figures 3I and 3K) since a supernatant from $Lp^{WCFS1} \Delta dhDL$ culture fails to accelerate development of larvae mono-associated with Ap^{WJL} (Figure 3M).

So far, we demonstrated that the positive effect of *L. plantarum* supernatant on larva mono-associated with Ap^{WJL} is based on its lactate content. Importantly, treatment of GF larvae with the supernatants of either Lp^{WCFS1} or $Lp^{WCFS1} \Delta dhDL$ has no effect on GF larvae development, neither does treatment with a supernatant of Ap^{WJL} grown either in the presence of these filtrates or with filtrates of Ap^{WJL} cocultured with any of the test *L. plantarum* strains (Figure S4G). Therefore, we first conclude that DL-lactate does not directly benefit the larval host, rather DL-lactate may trigger a switch of carbon utilization in Ap^{WJL} , which in turn reconfigures the metabolic by-products it releases, which the host utilizes to fuel its anabolic growth.

Lactate-Mediated Enhanced Ap^{WJL} Larval Growth Promotion Does Not Rely on Amino Acid Provision to the Host

To test our proposal, we focused on lactate metabolism in *A. pomorum*. Unfortunately, little is known about the core metabolism of this *Acetobacter* species. Most metabolic and genetic studies on *Acetobacter* have been performed on *A. acetii* because of its industrial use in vinegar production (Sakurai et al., 2010) or on *A. pasteurianus* as a core member of the fermenting microbiota of cocoa (Adler et al., 2014), which shares ~90% nucleotide identity with *A. pomorum* (Sannino et al., 2018). *A. pasteurianus* oxidizes lactate to pyruvate and converts it to (1) acetoin, which is released into the surrounding media, to (2) acetyl-CoA, which is directed to the TCA cycle, or (3) to phosphoenolpyruvate (PEP) for gluconeogenesis. In the two last cases, lactate consumption is accompanied by higher metabolic fluxes through biosynthetic pathways for biomass production including *de novo* amino acid biosynthesis (Adler et al., 2014).

We thus wondered if lactate consumption by Ap^{WJL} triggers an increased production and release of amino acids that would be consumed by the host and would stimulate larval growth. To test this hypothesis, we set cultures in liquid HD with or without DL-lactate supplementation, followed bacterial counts, and sampled supernatants every 24 h for 72 h for quantification of amino acids. We calculated the net amino acid release in each condition at 24, 48, and 72 h by subtracting the amino acid concentration quantified at 0 h from each incremental time points (Figures 4A and 4B). First, we observed a distinct release of amino acids at 24 and 48 h in both conditions. In the absence of lactate, we focused on the amino acid release by Ap^{WJL} at 48 h, while in the middle of its exponential phase (Figure 4A inner panel). With DL-lactate addition (Figure 4B), we observed a distinct release of amino acids at 24 (early exponential phase) and 48 h (late exponential phase, Figure 4B inner panel). Unexpectedly, during the stationary phase at 72 h, amino acids are depleted instead of accumulating.

Based on these observations, we prepared solid HDs each supplemented with the specific concentration of amino acid mixtures from each specific time points (Table S1; See Methods). These include a mixture of the amino acids representative of those released by Ap^{WJL} in liquid HD at 48 h (AA mix Ap @48h) and the mixtures of the amino acids released by Ap^{WJL} at 24 and 48 h in liquid HD supplemented with DL-lactate (AA mix Ap + lactate @24h and AA mix Ap + lactate @48h, respectively) (Figure 4B and inner panel). We then assessed the maturation time of GF and Ap^{WJL} mono-associated larvae on these three supplemented diets. We observe no enhanced benefit of the different amino acid mixes on GF or Ap^{WJL} mono-associated larvae maturation time (Figures 4C and 4D).

These results suggest that amino acid release by Ap^{WJL} is not a key mechanism by which Ap^{WJL} promotes host growth on complete HD, but we cannot rule out the contribution of amino acid precursors or derivatives to host growth promotion in this setting. However, our results indicate that the enhanced beneficial effect of Ap^{WJL} on larval development upon DL-lactate metabolism is not mediated by *de novo* amino acid biosynthesis and release.

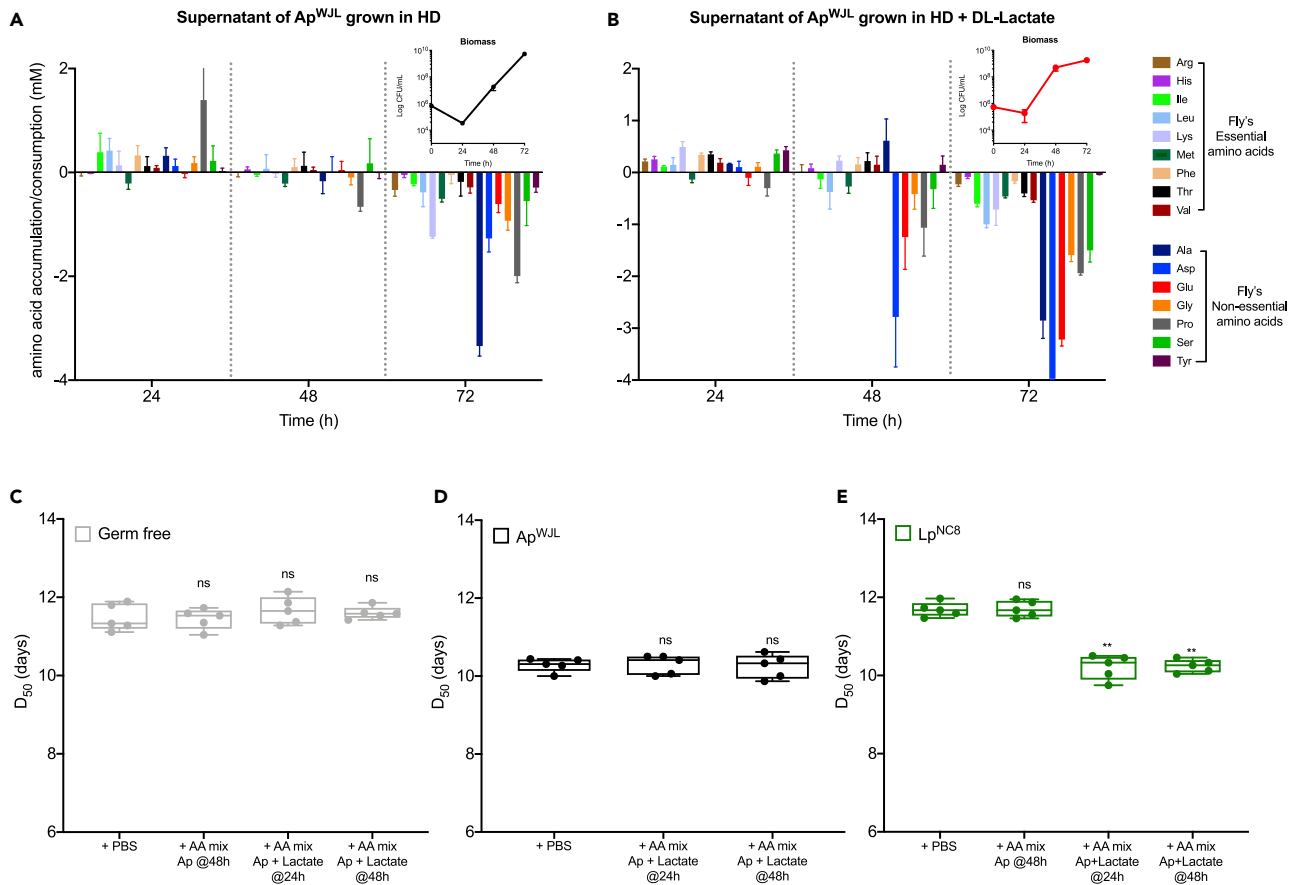


Figure 4. Upon Lactate Consumption Ap^{WJL} Produces an Amino Acid Cocktail that Enhances the Growth-Promoting Ability of Lp^{NC8}

(A and B) Net production of essential and non-essential fly amino acids at 24, 48, and 72 h. Net production was calculated from HPLC quantification data by subtracting the amino acid concentration quantified at 0 h from each incremental time point. Conditions included the supernatant of Ap^{WJL} cultures (inner panels) in complete HD supplemented (B) or not (A) with DL-lactate. Symbols in inner panels represent the means \pm SEM of three biological replicates. Bars represent the means \pm SEM of three biological replicates.

(C–E) Developmental timing of GF larvae (C) inoculated with 10^5 CFU of Ap^{WJL} (D) or 10^5 CFU of Lp^{NC8} (E) supplemented with either sterile PBS, the amino acid mix produced by Ap^{WJL} in liquid culture at 48 h (+AA mix Ap @48h), the amino acid mix produced by Ap^{WJL} in liquid culture supplemented with DL-lactate at 24 h (+AA mix Ap + Lactate @24h) or the amino acid mix produced by Ap^{WJL} in liquid culture supplemented with DL-lactate at 48 h (+AA mix Ap + Lactate @48h). See Table S1 for detailed information on the amino acid mixes. Boxplots show minimum, maximum, and median; each point represents a biological replicate. We performed Kruskal-Wallis test followed by uncorrected Dunn’s tests to compare each condition with the PBS-treated condition. ns: non-significant, **: p value < 0.005.

Upon Lactate Consumption Ap^{WJL} Produces Amino Acids that Enhance the Growth-Promoting Ability of Lp^{NC8}

We previously established that Ap^{WJL} cross-feeds amino acids and B vitamins to Lp^{NC8} (Figure 2). Therefore, we wonder if the amino acid mix produced by Ap^{WJL} while growing on HD supplemented with DL-lactate would further enhance the larval growth promotion ability of Lp^{NC8} . We tested this hypothesis in the same set-up described above (Figures 4A–4D). We prepared solid HDs supplemented with the three different mixtures of amino acids (AA mix Ap @48h; AA mix Ap + lactate @24h, and AA mix Ap + lactate @48h; Table S1). On these three supplemented media, the development of Lp^{NC8} mono-associated larvae is significantly accelerated with either the AA mix Ap + lactate @24h or AA mix Ap + lactate @48h but not with the AA mix Ap @48h (Figure 4E).

Together our results indicate that, upon consumption of the DL-lactate secreted by Lp^{NC8} , Ap^{WJL} releases amino acids that are now accessible to Lp^{NC8} . As a result, these amino acids further benefit Lp^{NC8} and enhance Lp^{NC8} -mediated larval growth promotion in complete HD. However, the amino acids released by Ap^{WJL} in response to lactate do not directly influence the host. This is therefore the metabolic cooperation between the two

commensals that results in increased host juvenile growth, higher microbial larval loads (Figures 1D and 1E), and improved growth rate of Ap^{WJL} and Lp^{NC8} in the HD (Figures 1F and 1G). These results establish that the metabolic cooperation occurring between the two major commensal bacteria of *Drosophila* supports an optimal nutritional mutualism among all the partners while facing amino acid scarcity.

Lactate Utilization by *Acetobacter* Is Necessary to Its Physiological Response to Lp^{NC8} and Enhanced Benefit on Host Growth

We aimed to elucidate the mechanisms underpinning the *Lactobacillus*-derived lactate influence on *Acetobacter* in relation to its increased potential to mediate larval growth. First, we focused on lactate utilization by *Acetobacter*. As mentioned previously, DL-lactate consumption by *A. pastorianus* generates acetoin and an increased carbon flux toward gluconeogenic pathways. These metabolic features seem to be shared among other *Acetobacter* species such as *A. fabarum*^{DsW_054} (Af), a strain isolated from wild-caught *Drosophila suzukii* (Winans et al., 2017). Indeed, Sommer and Newell recently reported that lactate produced by *L. brevis* is metabolized by Af through gluconeogenesis pathways via lactate dehydrogenase (LDH) and pyruvate phosphate dikinase (PPDK), whereas pyruvate is converted to acetoin by α -acetolactate synthase (ALS) and α -acetolactate decarboxylase (ALDC) (Sommer and Newell, 2018) (Figure 5A). Based on this information, we hypothesized that the effect of DL-lactate on Ap^{WJL} and the development of Ap^{WJL} mono-associated larvae relies on the lactate utilization by Ap^{WJL} and its conversion to acetoin or to an increased flux toward gluconeogenic pathways (Figure 5A). To test these hypotheses, we use a set of Af mutants affecting key enzymes of the lactate metabolism from the Af's transposon insertion mutant library generated by White et al. (2018) (Figure 5A). First, we confirmed that in HD Af behaves like Ap^{WJL} . As Ap^{WJL} , Af tends to accelerate larval development and Lp^{NC8} supernatant or DL-lactate supplementation enhances the influence of Af on larval growth (Figures 5B and 5C). As Ap^{WJL} , Af also consumes exogenous sources of DL-lactate, without a preference for either chiral form (Figure S5A). Af prevents the accumulation of DL-lactate produced by Lp^{NC8} when cocultured with this strain in liquid HD (Figure S5B). The first step of lactate metabolism is its oxidation by the enzyme LDH to produce two H^+ and pyruvate (Figure 5A). We tested two independent Af mutants in the *ldh* gene, Af::Tn*ldh*, clones 10B7 and 92G1 (Sommer and Newell, 2018; White et al., 2018). These mutants grow in liquid HD to the same extent as that of the Af wild-type strain (Figure S5C). On an HD supplemented with DL-lactate, Af::Tn*ldh* mutants consume the D chiral form of lactate (D-lactate) (Figures S5D and S5E) and still confer a significant benefit to larvae development upon addition of either DL-lactate or D-lactate, albeit with a slight reduction as compared with the WT strain (Figure 5C). However, both Af::Tn*ldh* mutants fail to consume L-lactate (Figures S5D and S5E) and accordingly completely fail to enhance larvae development upon addition of L-lactate (Figure 5C). These results therefore establish that the positive effect of lactate on the development of *Acetobacter* mono-associated larvae relies on lactate utilization by *Acetobacter* strains.

Acetobacter Acetoin Pathway Is Not Limiting for Lactate-Mediated Enhancement of *Acetobacter* Larval Growth Promotion

After LDH conversion of lactate to pyruvate, acetoin can be produced from pyruvate either directly through pyruvate decarboxylase (PDC) or by the successive action of ALS and ALDC with acetolactate as the intermediate product (Figure 5A). To investigate if the acetoin production pathway is necessary for the lactate-mediated enhancement of *Acetobacter* benefit to larvae development, we assessed the development of larvae mono-associated with each of the acetoin pathway mutants, Af::Tn*pdh*, Af::Tn*als*, and Af::Tn*aldc*, supplemented with DL-lactate. Of note, the mutants do not show any growth impairment on liquid HD (Figure S5F), and previous analyses of these mutants showed that, even if acetoin production is significantly reduced, it is not fully inhibited; the Af::Tn*als* and Af::Tn*aldc* mutants produce three times less acetoin than Af and Af::Tn*pdh* in rich liquid media (Sommer and Newell, 2018). However, all the mutants in the genes responsible for acetoin production enhance larval development upon addition of DL-lactate to the same extent as the WT strain (Figure 5D). Therefore, we conclude that acetoin production is not a limiting metabolic step in Af for the positive effect of lactate on the development of Af mono-associated larvae.

Another possible utilization of lactate by *Acetobacter* strains is the conversion from pyruvate to phosphoenolpyruvate (PEP) by the enzyme PPDK (Figure 5A). PEP is a precursor for the synthesis of many cellular building blocks through the gluconeogenesis and the pentose phosphate pathways. We hypothesize that DL-lactate consumption by Af results in a higher flux toward biosynthetic pathways. However, Tn disruption of the *ppdk* gene has a strong effect on Af fitness in HD, completely precluding the growth of the mutant strains in this media (Figure S5G) making it impossible to test them in our setting to obtain a complete genetic characterization of the phenotype.

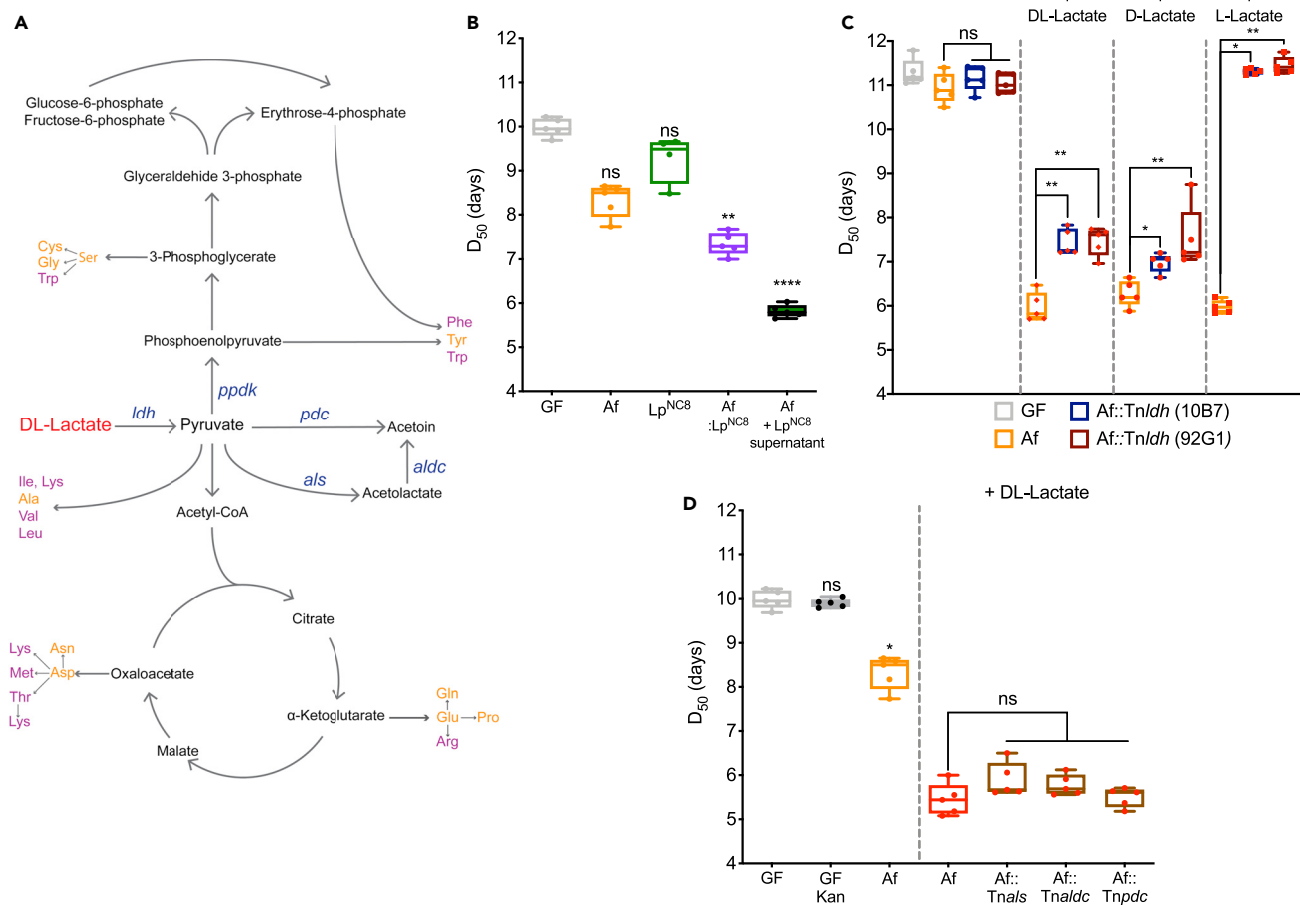


Figure 5. Lactate Utilization by *Acetobacter* Is Central to Its Physiological Response to Lp^{NC8} and Enhanced Benefit on Host Growth

(A) Schematic representation of the main metabolic routes of DL-lactate utilization by *Acetobacter* species. Purple: Fly's essential amino acids. Yellow: Fly's non-essential amino acids. Blue: genes related with lactate consumption.

(B) Developmental timing of Germ-Free (GF, gray) larvae or GF larvae inoculated with 10^5 CFU of *A. fabarum*^{D_{5W}_054} (Af, orange), Lp^{NC8} (green), both strains (Af: Lp^{NC8} , purple), or Af supplemented with the supernatant from 72-h culture of Lp^{NC8} (black, filled green) in complete HD.

(C) Developmental timing of GF (gray) larvae or GF larvae inoculated with 10^5 CFU of Af (orange), Af::Tnldh (10B7) (blue) or Af::Tnldh (92G1) (brown) supplemented with sterile PBS, DL-lactate, D-lactate, or L-lactate in complete HD.

(D) Developmental timing of GF (gray) larvae or GF larvae inoculated with 10^5 CFU of Af (orange) or Af (red), Af::Tnals (brown), Af::Tnaldc (brown), Af::Tnpdc (brown) supplemented with DL-lactate in complete HD or complete HD supplemented with 50 μ g/mL of kanamycin (GF and Af mutants). Boxplots show minimum, maximum, and median; each point represents a biological replicate. We performed Kruskal-Wallis test followed by uncorrected Dunn's tests to compare each condition with the GF treated condition or the Af condition when indicated. ns: non-significant, *: p value < 0.05, **: p value < 0.005, ****: p value < 0.0001.

See also Figure S5.

Lactate-Dependent *Acetobacter* Stimulation of Larval Growth Evokes Metabolites Release Enhancing Host Anabolic Metabolism and Resistance to Oxidative Stress

We next sought to characterize the molecular mechanisms involved in the enhancement of the growth promoting effect of *Acetobacter* strains upon lactate supplementation by a metabolic approach, using untargeted metabolomics (Figure 6). To this end, we used Af as a model bacterium since it reproduces the phenotype of Ap^{WJL} and Af's loss-of-function mutant Af::Tnldh (clone 10B7). We capitalized on these two strains to characterize the bacterial metabolites produced at day 3 upon L-lactate supplementation in the absence or presence of *Drosophila* larvae on HD (Figure 6A and see Methods). We chose this time point to collect the samples because at day 3 post mono-association and lactate supplementation, we start observing significant larval size gains when compared with GF or *Acetobacter* mono-associated larvae. Also, at this time point larvae are actively increasing their size and mass and have not yet reached the critical weight to enter metamorphosis (Figure 1B).

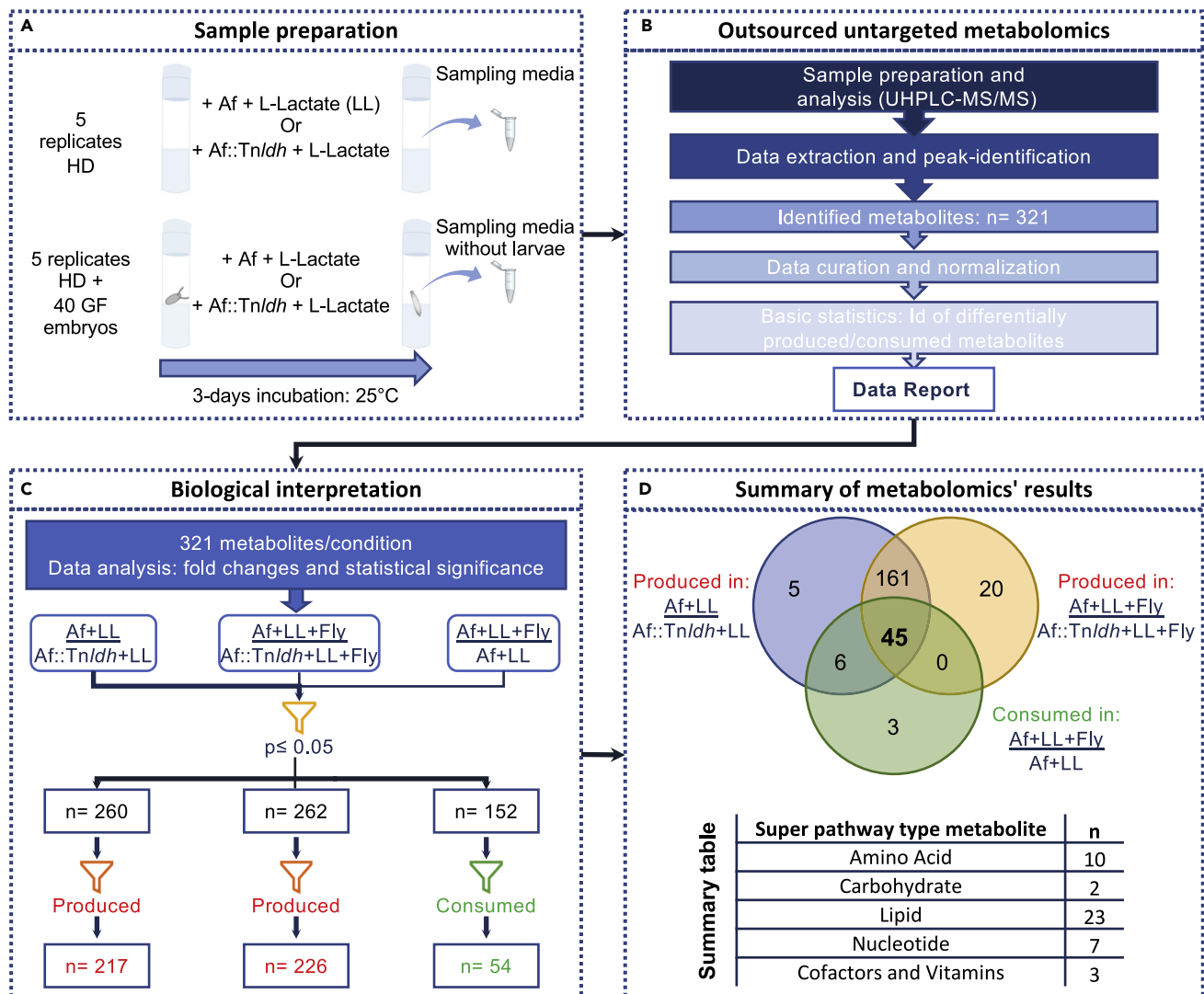


Figure 6. Lactate-Dependent Acetobacter Stimulation of Larval Growth Evokes Metabolites Release Enhancing Host Anabolic Metabolism and Resistance to Oxidative Stress

(A) Schematic representation of sample preparation for metabolomic analysis.

(B) Outsourced untargeted metabolomics and data analysis pipeline.

(C) Investigator-driven data analysis and biological interpretation.

(D) Venn diagram of the identified metabolites in the three test conditions. Our analysis points to 45 metabolites of interest belonging to all major metabolite families. See [Table 1](#) for a detailed list of metabolites.

Untargeted metabolomic analyses based on ultrahigh-performance liquid chromatography coupled to tandem mass spectrometry (UHPLC-MS/MS) identified 321 different metabolites (Figure 6B). We first calculated the fold changes of the metabolites among four conditions: Af + LL/Af::Tn/dh + LL, Af + LL + Fly/Af::Tn/dh + LL + Fly, and Af + LL + Fly/Af + LL (Figure 6C and Table S2). As shown above, Af::Tn/dh fails to consume L-lactate and does not accelerate larval development (Figures 5C, 5D, and 5E). Thus, the first two comparisons allow us to identify the differentially produced/consumed metabolites by Af upon L-lactate supplementation in the absence or presence of the larvae, respectively. The third comparison, Af + LL + Fly/Af + LL, allows us to identify the metabolites that are produced/consumed by the larvae when they are mono-associated with Af and supplemented with L-lactate. From the three different sets of differentially produced/consumed metabolites, we selected only the metabolites that differed with statistical significance between experimental groups (Welch's two-sample t test, $p \leq 0.05$, Figure 6C and Table S2). Next, we filtered the datasets in order to retain only the metabolites differentially produced by Af in

Super Pathway	Sub Pathway	Biochemical Name	Fold Change (p < 0.05)		
			$\frac{Af + LL}{Af::Tnldh + LL}$	$\frac{Af + LL + Fly}{Af::Tnldh + LL + Fly}$	$\frac{Af + LL + Fly}{Af + LL}$
Amino acid	Lysine metabolism	Pipecolate	228.86	1119.99	0.79
	Tryptophan metabolism	Indoleacetate	5.85	6.22	0.86
	Methionine, cysteine, SAM and taurine metabolism	S-adenosylmethionine (SAM)	2.94	1.64	0.56
		S-adenosylhomocysteine (SAH)	3.26	2.11	0.65
		Homocysteine	9.84	7.28	0.65
		Cysteine	8.31	5.87	0.85
		S-methylcysteine	14.10	7.95	0.54
	Polyamine metabolism	Spermidine	373.79	92.21	0.25
	Glutathione metabolism	Cysteinylglycine	4.22	1.43	0.34
Cys-gly, oxidized		15.23	1.92	0.13	
Carbohydrate	Glycolysis, gluconeogenesis, and pyruvate metabolism	Dihydroxyacetone phosphate (DHAP)	19.84	11.46	0.71
	Nucleotide sugar	UDP-glucuronate	3.86	1.94	0.50
Lipid	Long-chain monounsaturated fatty acid	Eicosenoate (20:1)	12.07	3.27	0.48
	Fatty acid, monohydroxy	2-Hydroxypalmitate	9.68	4.99	0.42
		2-Hydroxystearate	31.57	13.87	0.38
		3-Hydroxylaurate	12.74	5.64	0.45
		3-hydroxymyristate	48.30	7.43	0.22
		3-Hydroxypalmitate	105.93	34.11	0.25
		3-Hydroxystearate	97.11	46.57	0.30
	Phosphatidylcholine (PC)	1-Palmitoyl-2-palmitoleoyl-GPC	8.34	2.33	0.28
		1-Palmitoyl-2-oleoyl-GPC	38.40	33.83	0.26
		1-Palmitoleoyl-2-oleoyl-GPC	8.79	1.62	0.18
		1-Stearoyl-2-oleoyl-GPC	67.53	17.79	0.26
		1,2-Dioleoyl-GPC	135.60	276.71	0.32
	Phosphatidylethanolamine (PE)	1,2-Dipalmitoyl-GPE	6.14	1.63	0.27
		1-Palmitoyl-2-oleoyl-GPE	100.32	84.04	0.27
		1-Palmitoyl-2-linoleoyl-GPE	10.83	1.91	0.18
		1-Stearoyl-2-oleoyl-GPE	5.66	1.49	0.26
		1,2-Dioleoyl-GPE	156.95	77.19	0.29
	Phosphatidylglycerol (PG)	1,2-Dipalmitoyl-GPG	13.29	2.55	0.19

Table 1. Final Metabolite Candidate Set

(Continued on next page)

Super Pathway	Sub Pathway	Biochemical Name	Fold Change (p < 0.05)		
			Af + LL Af::Tnldh + LL	Af + LL + Fly Af::Tnldh + LL + Fly	Af + LL + Fly Af + LL
		1-Palmitoyl-2-oleoyl-GPG	4.75	1.43	0.30
		1-Stearoyl-2-oleoyl-GPG	4.10	1.38	0.34
		1,2-Dioleoyl-GPG	3.55	1.35	0.38
	Sphingolipid synthesis	Sphinganine	236.83	651.75	0.36
		Hexadecaspheganine	676.50	312.83	0.37
Nucleotide	Purine metabolism, adenine containing	Adenosine 5'-monophosphate (AMP)	264.58	146.97	0.32
		N6-methyladenosine	16.48	8.33	0.63
		guanosine 5'-monophosphate (5'-GMP)	12.58	4.64	0.37
	Pyrimidine metabolism, orotate containing	Dihydroorotate	17.16	10.60	0.65
		Uridine 5'-monophosphate (UMP)	11.18	2.82	0.25
		2'-Deoxyuridine	8.17	3.80	0.47
	Purine and pyrimidine metabolism	Methylphosphate	10.28	6.04	0.36
Cofactors and vitamins	Nicotinate and nicotinamide metabolism	Nicotinamide adenine dinucleotide (NAD+)	5.32	1.53	0.29
	Riboflavin metabolism	Flavin mononucleotide (FMN)	3.24	1.42	0.44
	Vitamin B6 metabolism	Pyridoxamine phosphate	5.02	1.93	0.38

Table 1. Continued

the absence or presence of the larvae upon L-lactate supplementation and the metabolites differentially consumed by the larvae in these conditions. The filtering generated three different sets of metabolites. The first is composed of 217 metabolites that are produced by Af upon L-lactate supplementation when growing on HD. The second comprises 226 metabolites that are produced by Af upon L-lactate supplementation when growing on HD in the presence of larvae. The third includes 54 metabolites that are consumed by larvae when mono-associated with Af and supplemented with L-lactate (Figure 6C and Table S2). Finally, we crossed the three sets of metabolites in order to retain only the metabolites that are produced by Af upon L-lactate supplementation in the presence or absence of larvae and that at the same time are consumed by the larvae (Figure 6D, Venn diagram). These analyses provide us with a set of 45 metabolites encompassing all main metabolite families such as amino acids, carbohydrates, lipids, nucleotides, co-enzymes, cofactors, and vitamins with a clear overrepresentation of amino acid derivatives and phospholipids (Figure 6D, summary table and Table 1).

The 45 differentially produced metabolites constitute a large repertoire of molecules produced by *Acetobacter* upon lactate utilization and are potentially accessible to the developing larvae. This particular combination of metabolites contains essential building blocks and regulators for the host's core anabolic process (nucleotides: AMP, GMP, UMP and cofactors/vitamins: NAD+, FMN, pyridoxamine phosphate) as well as regulator or intermediates of metabolic and developmental pathways (co-enzymes: SAM and SAH; phospholipids: biosynthetic intermediates of phosphatidylcholine, phosphatidylethanolamine, and phosphatidylglycerol pathways; and sphingolipids: sphinganine) and effectors of oxidative stress resistance (spermidine, cysteinylglycine). The collective action of these metabolites may converge to sustain linear larval growth and development despite a suboptimal nutritional environment. Altogether our work

identifies a fruitful metabolic cooperation among commensal bacteria that support their physiology and would boost host juvenile growth while facing amino acids scarcity.

DISCUSSION

Here, we identify a beneficial metabolic dialogue among frequently co-habiting species of *Drosophila*'s commensal bacteria that optimizes host juvenile growth and enables cross-feeding and nutrient provision upon chronic amino acid scarcity. Such benefit is also observed in full HDs containing optimal amino acid content as well as in fruit-based diets indicating that the metabolic cooperation among commensal bacteria and their influence on host growth is not restricted to artificial or poor nutritional conditions.

Using low amino acids-containing HDs as an experimental model, we show that *L. plantarum* captures the essential amino acids and B vitamins synthesized by the *Acetobacter* species to fulfill its auxotrophic requirements. In parallel, *Acetobacter* species exploit the lactate produced by *L. plantarum* as an additional carbon source that alters its metabolic state and physiology. Such metabolic interactions support an optimized growth of both commensal species in the diet and an increased colonization of the host.

Previous work has shown a positive correlation between host-associated microbial counts and linear larval growth in *Drosophila* (Keebaugh et al., 2019). Moreover, inert microbial biomass (heat-killed microbes) can accelerate larval development (Bing et al., 2018; Storelli et al., 2011) and impact *Drosophila* lifespan (Yamada et al., 2015). Here, we show that the metabolic cooperation between Ap^{WJL} and Lp^{NC8} increases bacterial biomass in the nutritional substrate, which slightly increases larval growth. However, the bacterial biomass alone never reproduces to the same extent as the positive impact of live $Ap^{WJL}:Lp^{NC8}$ bi-association or lactate supplemented Ap^{WJL} mono-association on host growth. Instead, we show that lactate utilization by *Acetobacter* species rewires its carbon metabolism resulting in the enhanced and *de novo* production of a panoply of anabolic metabolites that would support enhanced host systemic growth.

Studies have previously shown that cooperation among the gut microbes can influence other aspects of *Drosophila* physiology. For example, multiple fermentation products of *L. brevis* foster the growth of *A. fabarum* on a fly diet leading to depletion of dietary glucose, consequently triggering reduced TAG levels in the adult host (Newell and Douglas, 2014; Sommer and Newell, 2018). Moreover, multi-microbe interactions among the *Acetobacter* and *Lactobacillus* species and yeast were shown to influence additional adult traits such as olfaction and egg laying behavior (Fischer et al., 2017), food choice behavior (Leitão-Gonçalves et al., 2017), lifespan and fecundity (Gould et al., 2018), and immunity (Fast et al., 2020). Therefore, along with these studies, our work provides an entry point to further deepen the understanding of how metabolites originating from microbial metabolic networks shape the biology of their host.

In this study, we confirm that lactate is a key metabolite supporting the metabolic cross talk between different microbial species. Lactate supplementation to *Acetobacter* species triggers the release of metabolic by-products that include ribonucleotides AMP, GMP, and UMP and vitamin and amino acid derivatives SAM, SAH, NAD^+ , FMN, and pyridoxamine phosphate, which are co-factors for enzymes involved in multiple host metabolic pathways. These metabolites are essential for optimal larval growth and survival (Consuegra et al., 2020; Mishra et al., 2018; Sang, 1956). Fatty acids and membrane lipids are another group of metabolites whose production is enhanced by lactate presence. Among this group, we found mostly phospholipids such as phosphatidylcholine (PC), phosphatidylethanolamine (PE), and phosphatidylglycerol (PG) and a sphingolipid precursor, sphinganine. In *Drosophila*, PE, PC, PG, and sphingolipids are part of the membrane phospholipids repertoire, with PE being the largely dominating species (Carvalho et al., 2012). Previously, it was established that the total content of membrane lipids increases during larval growth, until a clear pause that occurs in the third instar just prior to the time when larvae stop feeding and enter the wandering stage. This indicates that feeding larvae favor new membrane synthesis and tissue growth over lipid storage (Carvalho et al., 2012). In the same study, it was shown that dietary lipids directly influence membrane lipids proportions, including phospholipids and sphingolipids. In mammals, sphingolipid balance has a central role in controlling nutrient utilization and growth (Holland et al., 2007). Sphingolipids are also activators of serum response element binding protein signaling, which controls biosynthesis of fats (Worgall, 2008). Despite a relatively smaller literature on *Drosophila* sphingolipids, these lipids seem as critical to developmental and metabolic processes in the fly as they are to mammals (Kraut, 2011). Although *Drosophila* cells can synthesize *de novo* all the fatty acids for survival, they incorporate different dietary lipids into the membrane lipids if found in the diet (Carvalho et al., 2012). Therefore, we propose that larvae preferentially utilize the PC, PE, PG, and sphingolipids intermediates produced by *Acetobacter*

species upon lactate utilization to foster membrane synthesis, tissue growth, and metabolic processes such as lipid storage and response to nutrient availability.

Lactate utilization also triggers another major class of metabolites released by *Acetobacter* species that confers oxidative stress resistance. Specifically, we found cysteinylglycine and spermidine. Cysteinylglycine is an intermediate of glutathione (GSH) metabolism, the most abundant cellular antioxidant (Forman et al., 2009). It is produced by GSH hydrolysis or by action of the enzyme γ -L-glutamyl-transpeptidase (GGT). GGT transfers the γ -glutamyl group of GSH onto amino acids forming γ -glutamyl peptides and cysteinylglycine. These intermediaries can be recycled and used to resynthesize GSH and maintain its cellular pool, which protects cells from oxidative damage and maintains redox homeostasis (Ursini et al., 2016). Of note, during *Drosophila* larval development, in addition to its antioxidant role, GSH also contributes to ecdysteroid biosynthesis including the biologically active hormone 20-hydroxyecdysone, which plays an essential role in promoting juvenile growth and maturation (Enya et al., 2017). Spermidine is a natural polyamine widely found in both prokaryotes and eukaryotes including flies and mammals. Nutritional supplementation of spermidine increases the lifespan of yeast, worms, flies, and human cells through inhibition of oxidative stress (Eisenberg et al., 2009). The mode of action of spermidine, mainly through autophagy regulation, is emerging, but evidence for other mechanisms exist such as inflammation reduction, lipid metabolism, and regulation of cell growth, proliferation, and death (Minois, 2014; Minois et al., 2012). Oxidative stress resistance in *Drosophila* has been largely reported to improve adult physiology including lifespan extension. We therefore posit that larvae's physiology and growth potential are also supported by such metabolites obtained from their microbial partners, especially during development on a suboptimal diet. Further work, including testing individual metabolites and their combinations, will be required to identify the specific compounds or cocktails produced by *Acetobacter* upon lactate utilization supporting acceleration of larval development.

Beyond essential nutrient provision and metabolic cooperation between commensals and their host, we posit that other bacteria-mediated mechanisms would also contribute to enhanced host growth. Indeed, upon lactate utilization *Acetobacter* may release molecules that would activate host endocrine signals and promote anabolism. Accordingly, it was recently shown that acetate produced by *Acetobacter* improves larval growth by impacting host lipid metabolism through the activation of the IMD signaling pathway in entero-endocrine cells and the release of the endocrine peptide tachykinin (Kamareddine et al., 2018). However, this mechanism is unlikely to be at play here owing to the high content of acetate in our fly diet.

Collectively our results deconstruct the intertwined metabolic networks forged between commensal bacteria that support juvenile growth of the host. This work contributes to the understanding of how the microbiota activities as a whole influence host nutritional and metabolic processes supporting host juvenile growth despite a stressful nutritional environment.

Limitations of the Study

The complete genetic characterization of Lactate-dependent *Acetobacter* stimulation of larval growth was hampered by the lethality of *Acetobacter* mutants affecting the central metabolic pathways while growing in complete HD. Instead, using metabolomics, we pinpoint a large repertoire of molecules produced by *Acetobacter* upon lactate utilization and accessible to the developing larvae. Further studies will be necessary to test the 45 candidate metabolites, individually or in combinations, to identify the minimal metabolite cocktail enhancing the development of GF larvae or larvae mono-associated with *Acetobacter*. Moreover, functional analyses in the host would be required to identify the metabolic pathways sustained by commensal bacteria and involved in the anabolic growth of the host.

Resource Availability

Lead Contact

Further information and requests for resources should be addressed to the Lead Contact, François Leulier (francois.leulier@ens-lyon.fr).

Materials Availability

This study did not generate new unique reagents.

Data and Code Availability

Tables 1 and S2 provide the main results derived from the metabolomic analysis presented in this study.

METHODS

All methods can be found in the accompanying [Transparent Methods supplemental file](#).

SUPPLEMENTAL INFORMATION

Supplemental Information can be found online at <https://doi.org/10.1016/j.isci.2020.101232>.

ACKNOWLEDGMENTS

We would like to thank Dali Ma for critical reading and editing of the manuscript and valuable suggestions, John Chaston and Peter Newell for *Acetobacter fabarum* strains and mutants, and the ArthroTools platform of the SFR Biosciences (UMS3444/US8) for fly equipment and facility. Research in F.L.'s lab is supported by the ENS de Lyon, CNRS, and the Finovi foundation. Research in P.d.S.' lab is supported by INRA and INSA Lyon. J.C. is funded by a postdoctoral fellowship from the "Fondation pour la Recherche Médicale" (FRM, SPF20170938612). T.G. is funded by a PhD fellowship from ENS de Lyon.

AUTHOR CONTRIBUTIONS

Conceptualization, J.C. and F.L.; Methodology, J.C. and F.L.; Validation, J.C. and F.L.; Formal Analysis, J.C.; Investigation, J.C., T.G., H.A., H.G., I.R., and P.d.S.; Data Curation, J.C.; Writing – Original Draft, J.C. and F.L.; Writing – Review & Editing, J.C. T.G., P.d.S., and F.L.; Visualization, J.C.; Supervision, J.C. and F.L.; Project Administration, J.C. and F.L.; Funding Acquisition, F.L.

DECLARATION OF INTERESTS

The authors declare no competing financial interests.

Received: November 12, 2019

Revised: March 13, 2020

Accepted: June 1, 2020

Published: June 26, 2020

REFERENCES

- Adler, P., Frey, L., Berger, A., Bolten, C., Hansen, C., and Wittmann, C. (2014). The key to acetate: metabolic fluxes of acetic acid bacteria under cocoa pulp fermentation-simulating conditions. *Appl. Environ. Microbiol.* *80*, 4702–4716.
- Bing, X., Gerlach, J., Loeb, G., and Buchon, N. (2018). Nutrient-dependent impact of microbes on *Drosophila suzukii* development. *mBio* *9*, e02199–17.
- Blanton, L.V., Charbonneau, M.R., Salih, T., Barratt, M.J., Venkatesh, S., Ilkaveya, O., Subramanian, S., Manary, M.J., Trehan, I., Jorgensen, J.M., et al. (2016). Gut bacteria that prevent growth impairments transmitted by microbiota from malnourished children. *Science* *351*, aad3311-1–aad3311-7.
- Carvalho, M., Sampaio, J.L., Palm, W., Brankatschk, M., Eaton, S., and Shevchenko, A. (2012). Effects of diet and development on the *Drosophila* lipidome. *Mol. Syst. Biol.* *8*, 600.
- Chandler, J.A., Lang, J.M., Bhatnagar, S., Eisen, J.A., and Kopp, A. (2011). Bacterial communities of diverse *Drosophila* species: ecological context of a host–microbe model system. *PLoS Genet.* *7*, e1002272.
- Consuegra, J., Grenier, T., Baa-Puyoulet, P., Rahioui, I., Akherraz, H., Gervais, H., Parisot, N., Silva, P., Charles, H., Calevro, F., et al. (2020). *Drosophila*-associated bacteria differentially shape the nutritional requirements of their host during juvenile growth. *Plos Biol.* *18*, e3000681.
- Development Initiatives (2018). 2018 Global Nutrition Report: Shining a light to spur action on nutrition (Development Initiatives).
- Eisenberg, T., Knauer, H., Schauer, A., Büttner, S., Ruckstuhl, C., Carmona-Gutierrez, D., Ring, J., Schroeder, S., Magnes, C., Antonacci, L., et al. (2009). Induction of autophagy by spermidine promotes longevity. *Nat. Cell. Biol.* *11*, ncb1975.
- Enya, S., Yamamoto, C., Mizuno, H., Esaki, T., Lin, H.-K., Iga, M., Morohashi, K., Hirano, Y., Kataoka, H., Masujima, T., et al. (2017). Dual roles of glutathione in ecdysone biosynthesis and antioxidant function during the larval development in *Drosophila*. *Genetics* *207*, 1519–1532.
- Fast, D., Petkau, K., Ferguson, M., Shin, M., Galenza, A., Kostiuik, B., Pukatzki, S., and Foley, E. (2020). *Vibrio cholerae*-symbiont interactions inhibit intestinal repair in *Drosophila*. *Cell Rep.* *30*, 1088–1100.
- Ferain, T., Hobbs, J.N., Richardson, J., Bernard, N., Garmyn, D., Hols, P., Allen, N.E., and Delcour, J. (1996). Knockout of the two *ldh* genes has a major impact on peptidoglycan precursor synthesis in *Lactobacillus plantarum*. *J. Bacteriol.* *178*, 5431–5437.
- Fischer, C., Trautman, E.P., Crawford, J.M., Stabb, E.V., Handelsman, J., and Broderick, N.A. (2017). Metabolite exchange between microbiome members produces compounds that influence *Drosophila* behavior. *Elife* *6*, e18855.
- Forman, H.J., Zhang, H., and Rinna, A. (2009). Glutathione: overview of its protective roles, measurement, and biosynthesis. *Mol. Aspects. Med.* *30*, 1–12.
- Gould, A.L., Zhang, V., Lamberti, L., Jones, E.W., Obadia, B., Korasidis, N., Gavryushkin, A., Carlson, J.M., Beerenwinkel, N., and Ludington, W.B. (2018). Microbiome interactions shape host fitness. *Proc. Natl. Acad. Sci. U S A* *115*, E11951–E11960.
- Goyal, M.S., Venkatesh, S., Milbrandt, J., Gordon, J.I., and Raichle, M.E. (2015). Feeding the brain and nurturing the mind: linking nutrition and the gut microbiota to brain development. *Proc. Natl. Acad. Sci. U S A* *112*, 14105–14112.
- Holland, W.L., Brozinick, J.T., Wang, L.-P., Hawkins, E.D., Sargent, K.M., Liu, Y., Narra, K., Hoehn, K.L., Knotts, T.A., Siesky, A., et al. (2007). Inhibition of ceramide synthesis ameliorates glucocorticoid-, saturated-fat-, and obesity-induced insulin resistance. *Cell Metab* *5*, 167–179.
- Hooper, L.V., and Gordon, J.I. (2018). Commensal host-bacterial relationships in the gut. *Science* *292*, 1115–1118.

- Jang, T., and Lee, K.P. (2018). Comparing the impacts of macronutrients on life-history traits in larval and adult *Drosophila melanogaster*: the use of nutritional geometry and chemically defined diets. *J. Exp. Biol.* 221, jeb181115.
- Kamareddine, L., Robins, W.P., Berkey, C.D., Mekalanos, J.J., and Watnick, P.I. (2018). The *Drosophila* immune deficiency pathway modulates enteroendocrine function and host metabolism. *Cell Metab.* 28, 1–14.
- Keebaugh, E.S., Yamada, R., Obadia, B., Ludington, W.B., and Ja, W.W. (2018). Microbial quantity impacts *Drosophila* nutrition, development, and lifespan. *iScience* 4, 247–259.
- Keebaugh, E.S., Yamada, R., and Ja, W.W. (2019). The nutritional environment influences the impact of microbes on *Drosophila melanogaster* life span. *mBio* 10, e00885–19.
- Kraut, R. (2011). Roles of sphingolipids in *Drosophila* development and disease. *J. Neurochem.* 116, 764–778.
- Leitão-Gonçalves, R., Carvalho-Santos, Z., Francisco, A.P., Fioreze, G.T., Anjos, M., Baltazar, C., Elias, A.P., Itskov, P.M., Piper, M.D.W., and Ribeiro, C. (2017). Commensal bacteria and essential amino acids control food choice behavior and reproduction. *Plos Biol.* 15, e2000862.
- Martino, M.E., Bayjanov, J.R., Caffrey, B.E., Wels, M., Joncour, P., Hughes, S., Gillet, B., Kleerebezem, M., van Hijum, S.A.F.T., and Leulier, F. (2016). Nomadic lifestyle of *Lactobacillus plantarum* revealed by comparative genomics of 54 strains isolated from different habitats. *Environ. Microbiol.* 18, 4974–4989.
- Matos, R.C., Schwarzer, M., Gervais, H., Courtin, P., Joncour, P., Gillet, B., Ma, D., Bulteau, A.-L., Martino, M., Hughes, S., et al. (2017). D-alanine esterification of teichoic acids contributes to *Lactobacillus plantarum* mediated *Drosophila* growth promotion upon chronic undernutrition. *Nat. Microbiol.* 2, 1635–1647.
- Minois, N. (2014). Molecular basis of the “anti-aging” effect of spermidine and other natural polyamines - a mini-review. *Gerontology* 60, 319–326.
- Minois, N., Carmona-Gutierrez, D., Bauer, M.A., Rockenfeller, P., Eisenberg, T., Brandhorst, S., Sigrist, S.J., Kroemer, G., and Madeo, F. (2012). Spermidine promotes stress resistance in *Drosophila melanogaster* through autophagy-dependent and -independent pathways. *Cell. Death Dis.* 3, e401.
- Mishra, D., Thorne, N., Miyamoto, C., Jagge, C., and Amrein, H. (2018). The taste of ribonucleosides: novel macronutrients essential for larval growth are sensed by *Drosophila* gustatory receptor proteins. *PLoS Biol.* 16, e2005570.
- Newell, P.D., and Douglas, A.E. (2014). Interspecies interactions determine the impact of the gut Microbiota on nutrient allocation in *Drosophila melanogaster*. *Appl. Environ. Microbiol.* 80, 788–796.
- Oyeyinka, B.O., and Afolayan, A.J. (2019). Comparative evaluation of the nutritive, mineral, and antinutritive composition of *Musa sinensis* L. (Banana) and *Musa paradisiaca* L. (Plantain) fruit compartments. *Plants* 8, 598.
- Pais, I.S., Valente, R.S., Sporniak, M., and Teixeira, L. (2018). *Drosophila melanogaster* establishes a species-specific mutualistic interaction with stable gut-colonizing bacteria. *PLoS Biol.* 16, e2005710.
- Piper, M.D.W., Blanc, E., Leitão-Gonçalves, R., Yang, M., He, X., Linford, N.J., Hoddinott, M.P., Hopfen, C., Soultoukis, G.A., Niemeier, C., et al. (2013). A holidic medium for *Drosophila melanogaster*. *Nat. Methods* 11, 100–105.
- Piper, M.D.W., Soultoukis, G.A., Blanc, E., Mesaros, A., Herbert, S.L., Juricic, P., He, X., Atanassov, I., Salmonowicz, H., Yang, M., et al. (2017). Matching dietary amino acid balance to the in Silico-translated exome optimizes growth and reproduction without cost to lifespan. *Cell Metab.* 25, 610–621.
- Rapport, E.W., Stanley-Samuelson, D., and Dadd, R.H. (1983). Ten generations of *Drosophila melanogaster* reared asexually on a fatty acid-free holidic diet. *Arch. Insect Biochem.* 1, 243–250.
- Sakurai, K., Arai, H., Ishii, M., and Igarashi, Y. (2010). Transcriptome response to different carbon sources in *Acetobacter acetii*. *Microbiology* 157, 899–910.
- Sang, J.H. (1956). The quantitative nutritional requirements of *Drosophila melanogaster*. *J. Exp. Biol.* 33, 45–72.
- Sannino, D.R., Dobson, A.J., Edwards, K., Angert, E.R., and Buchon, N. (2018). The *Drosophila melanogaster* gut microbiota provisions thiamine to its host. *mBio* 9, e00155–18.
- Schroeder, B.O., and Bäckhed, F. (2016). Signals from the gut microbiota to distant organs in physiology and disease. *Nat. Med.* 22, 1079–1089.
- Schultz, J., Lawrence, P.S., and Newmeyer, D. (1946). A chemically defined medium for the growth of *Drosophila melanogaster*. *Anatomical Rec.* 96, 540.
- Schwarzer, M., Makki, K., Storelli, G., Machuca-Gayet, I., Srutkova, D., Hermanova, P., Martino, M.E., Balmund, S., Hudcovic, T., Heddi, A., et al. (2016). *Lactobacillus plantarum* strain maintains growth of infant mice during chronic undernutrition. *Science* 351, 854–857.
- Shin, S., Kim, S.-H., You, H., Kim, B., Kim, A.C., Lee, K.-A., Yoon, J.-H., Ryu, J.-H., and Lee, W.-J. (2011). *Drosophila* microbiome modulates host developmental and metabolic homeostasis via insulin signaling. *Science* 334, 670–674.
- Smith, M.I., Yatsunenko, T., Manary, M.J., Trehan, I., Mkakosya, R., Cheng, J., Kau, A.L., Rich, S.S., Concannon, P., Mychaleckyj, J.C., et al. (2013). Gut microbiomes of Malawian twin pairs discordant for kwashiorkor. *Science* 339, 548–554.
- Sommer, A.J., and Newell, P.D. (2018). Metabolic basis for mutualism between gut bacteria and its impact on their host *Drosophila melanogaster*. *Appl. Environ. Microb.* 85, e01882–18.
- Storelli, G., Defaye, A., Erkosar, B., Hols, P., Royet, J., and Leulier, F. (2011). *Lactobacillus plantarum* promotes *Drosophila* systemic growth by modulating hormonal signals through TOR-dependent nutrient sensing. *Cell Metab.* 14, 403–414.
- Subramanian, S., Huq, S., Yatsunenko, T., Haque, R., Mahfuz, M., Alam, M., Benezra, A., DeStefano, J., Meier, M., Muegge, B., et al. (2014). Persistent gut microbiota immaturity in malnourished Bangladeshi children. *Nature* 510, 417–421.
- Thissen, J.-P., Ketelslegers, J.-M., and Underwood, L.E. (1994). Nutritional regulation of the insulin-like growth factors. *Endocr. Rev.* 15, 80–101.
- Ursini, F., Maiorino, M., and Forman, H.J. (2016). Redox homeostasis: the Golden Mean of healthy living. *Redox Biol.* 8, 205–215.
- P. Vos, G. Garrity, D. Jones, N.R. Krieg, W. Ludwig, F.A. Rainey, K.-H. Schleifer, and W. Whitman, eds (2009). *Bergey’s Manual of Systematic Bacteriology*, 2nd ed. The Firmicutes, Volume 3 (Springer-Verlag).
- White, K.M., Matthews, M.K., Hughes, R., Sommer, A.J., Griffiths, J.S., Newell, P.D., and Chaston, J.M. (2018). A metagenome-wide association study and arrayed mutant library confirm *Acetobacter* lipopolysaccharide genes are necessary for association with *Drosophila melanogaster*. *G3 (Bethesda)* 8, 1119–1127.
- Winans, N.J., Walter, A., Chouaib, B., Chaston, J.M., Douglas, A.E., and Newell, P.D. (2017). A genomic investigation of ecological differentiation between free-living and *Drosophila*-associated bacteria. *Mol. Ecol.* 26, 4536–4550.
- Wong, A.C.-N., Chaston, J.M., and Douglas, A.E. (2013). The inconstant gut microbiota of *Drosophila* species revealed by 16S rRNA gene analysis. *ISME J.* 7, 1922–1932.
- Worgall, T.S. (2008). Regulation of lipid metabolism by sphingolipids. *Subcell. Biochem.* 49, 371–385.
- Yamada, R., Deshpande, S.A., Bruce, K.D., Mak, E.M., and Ja, W.W. (2015). Microbes promote amino acid harvest to rescue undernutrition in *Drosophila*. *Cell Rep.* 10, 865–872.
- Yan, J., Herzog, J.W., Tsang, K., Brennan, C.A., Bower, M.A., Garrett, W.S., Sartor, B.R., Aliprantis, A.O., and Charles, J.F. (2016). Gut microbiota induce IGF-1 and promote bone formation and growth. *Proc. Natl. Acad. Sci. U S A* 113, E7554–E7563.

iScience, Volume 23

Supplemental Information

Metabolic Cooperation among Commensal Bacteria

Supports *Drosophila* Juvenile Growth

under Nutritional Stress

Jessika Consuegra, Théodore Grenier, Houssam Akherraz, Isabelle Rahioui, Hugo Gervais, Pedro da Silva, and François Leulier

without (C) larvae, from day 0 to 4 days and 8 days after inoculation. Boxplots show minimum, maximum and median. Points represent biological replicates. We performed Kruskal-Wallis test followed by uncorrected Dunn's tests to compare each condition to the GF treated condition. ns: non-significant, *: p-value<0,05, **: p-value<0,005, ***: p-value<0,0005 ****: p-value<0,0001. Dot plots shows mean and each dot represents an independent biological replicate.

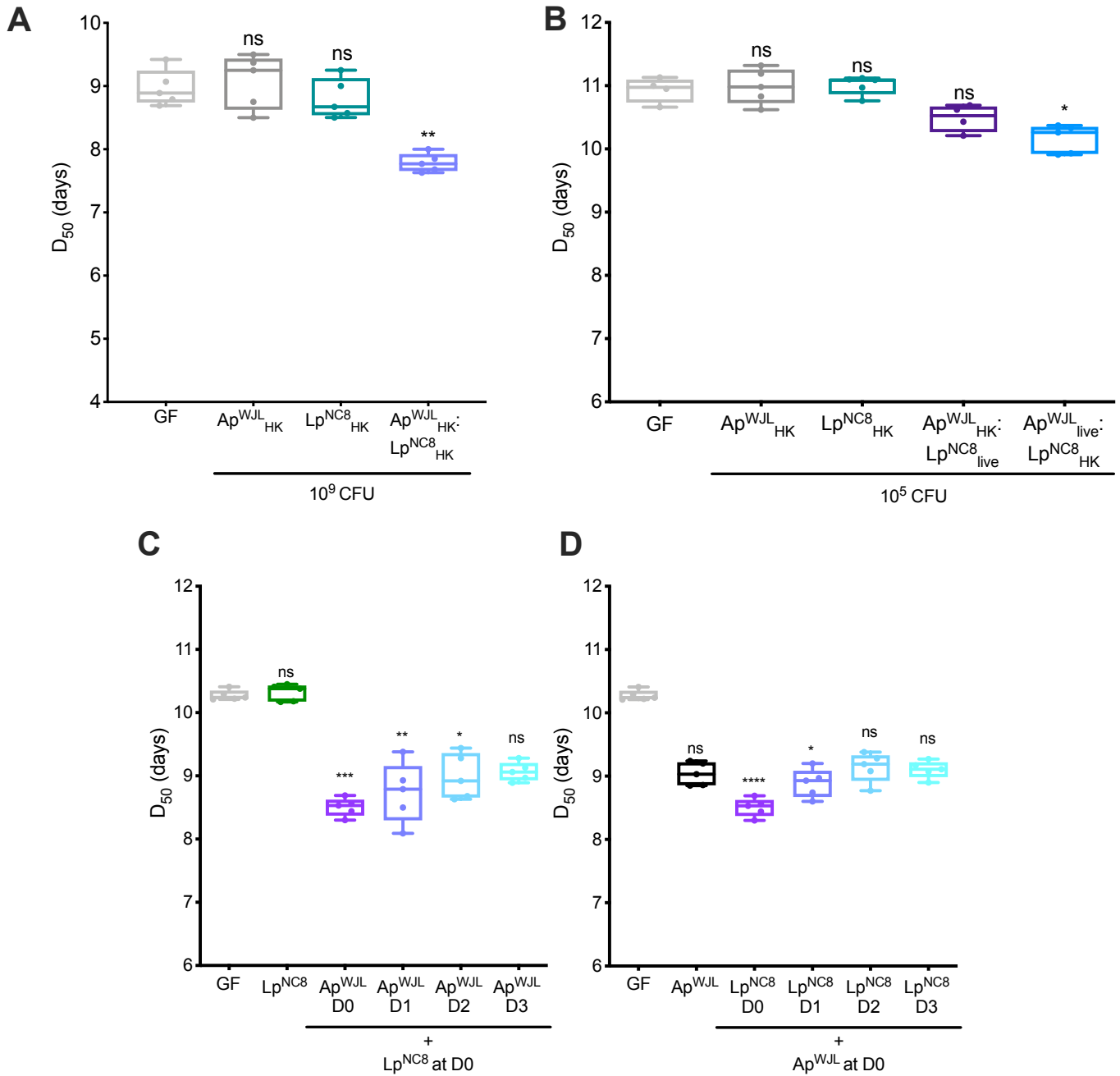


Figure S2. Related to Figure 1: (A) Developmental timing of Germ Free (GF, light grey) larvae or GF larvae inoculated with 10^9 CFU of Ap^{WJL} Heat-Killed (Ap^{WJL}_{HK} , dark grey), Lp^{NC8}_{HK} (turquoise) or $Ap^{WJL}_{HK} : Lp^{NC8}_{HK}$ bi-association (light purple). (B) Developmental timing of GF (light grey) larvae or GF larvae inoculated with 10^5 CFU of Ap^{WJL}_{HK} (dark grey), Lp^{NC8}_{HK} (turquoise), Ap^{WJL}_{HK} plus live Lp^{NC8} ($Ap^{WJL}_{HK} : Lp^{NC8}_{live}$, dark purple) or $Ap^{WJL}_{live} : Lp^{NC8}_{HK}$, light blue). (C) Developmental timing of GF (grey)

larvae or GF larvae inoculated with 10^5 CFU of Lp^{NC8} at D0 and subsequently at D0/1/2/3 with $\sim 10^5$ CFU of Ap^{WJL} . (D) Developmental timing of GF (grey) larvae or GF larvae inoculated with 10^5 CFU of Ap^{WJL} at D0 and subsequently at D0/1/2/3 with 10^5 CFU of Lp^{NC8} . Boxplots show minimum, maximum and median. Points represent biological replicates. We performed Kruskal-Wallis test followed by uncorrected Dunn's tests to compare each condition to the GF treated condition. ns: non-significant, *: p-value<0,05, **: p-value<0,005, ***: p-value<0,0005 ****: p-value<0,0001.

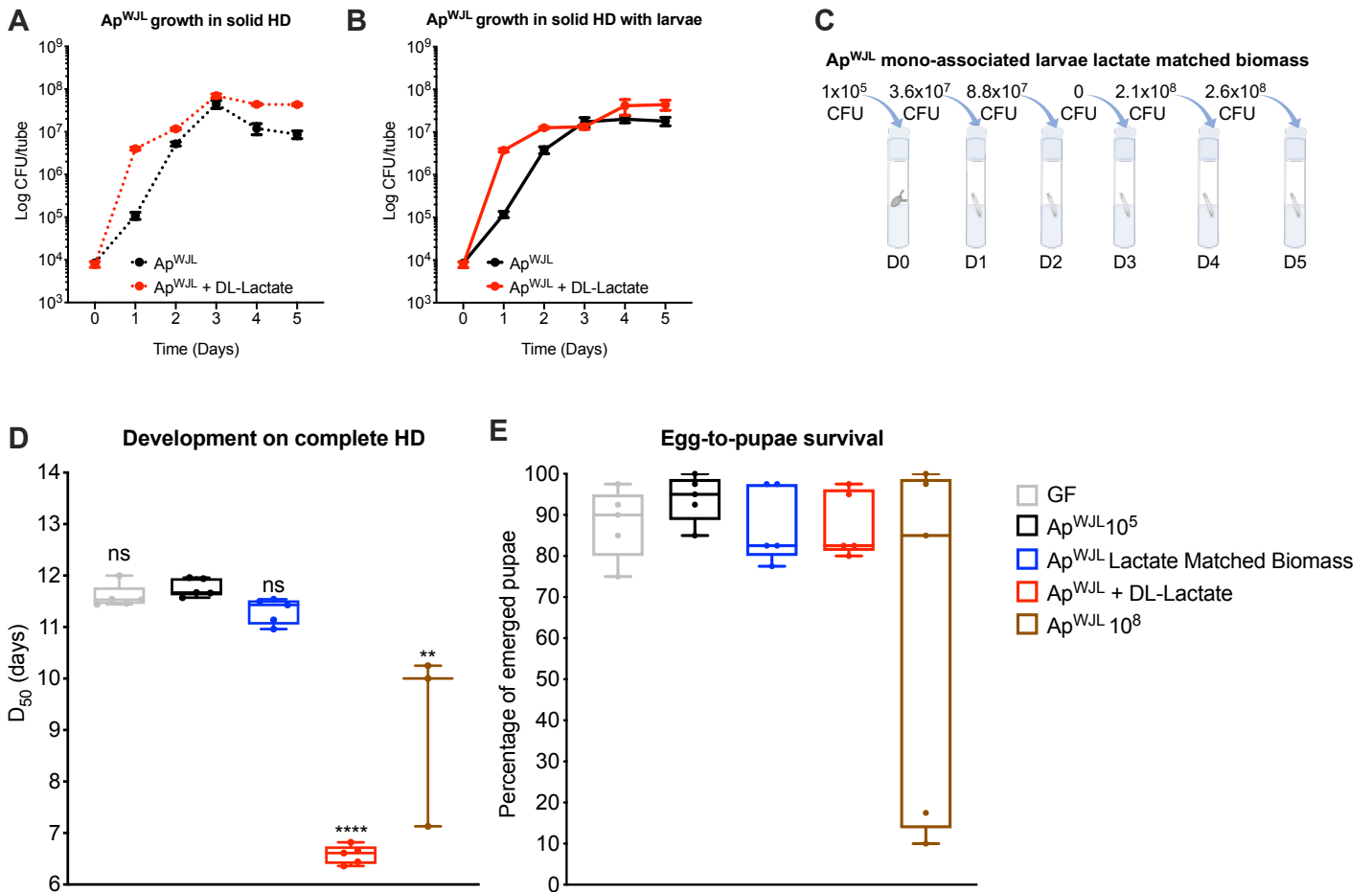


Figure S3. Related to Figure 3: (A-B) Load of Ap^{WJL} in solid HD supplemented (red) or not (black) with DL-lactate at a final concentration of 0.6 g/L with (B) and without (A) larvae, from day 0 to 5 days after inoculation. (C) Graphical representation of the daily Ap^{WJL} biomass supplementation to Ap^{WJL} mono-associated larvae in order to match the biomass reached upon DL-lactate supplementation, according with Fig. S3B. (D) Developmental timing of Germ Free (GF, light grey) larvae or GF larvae inoculated with 10^5 CFU of Ap^{WJL} (black) or Ap^{WJL} mono-associated larvae supplemented daily with live Ap^{WJL} biomass (blue) or DL-lactate (red) and GF larvae inoculated with 10^8 CFU of Ap^{WJL} (brown). (E) Percentage of the emerged pupae from the developmental timing experiment of Fig. S3D. Symbols represent the means \pm SEM of three biological replicates except for panel (A-B). Boxplots show minimum, maximum and median. Points represent biological replicates. We performed Kruskal-Wallis test followed by

uncorrected Dunn's tests to compare each condition to the GF treated condition. ns: non-significant, *: p-value<0,05, **: p-value<0,005, ***: p-value<0,0005 ****: p-value<0,0001.

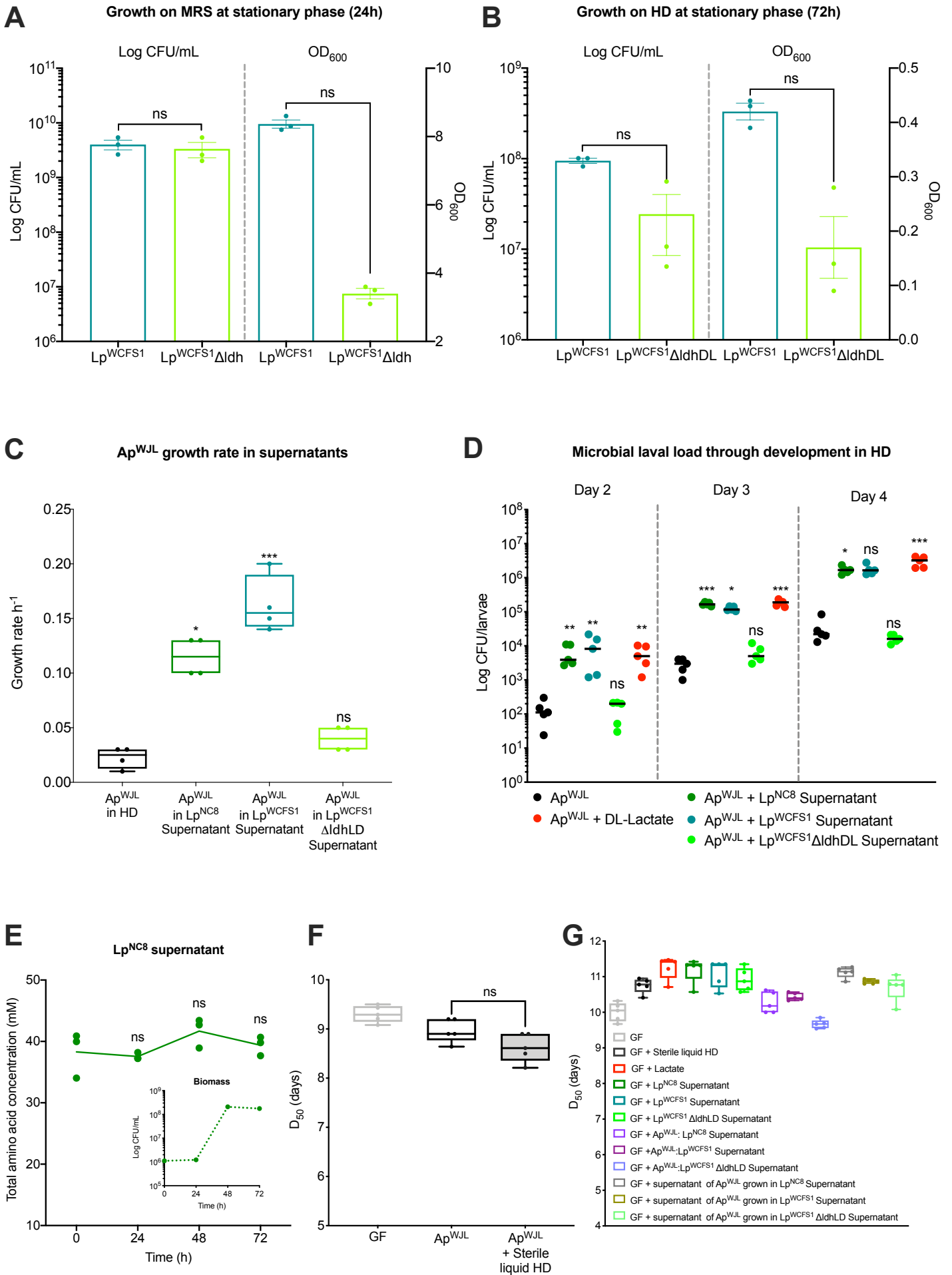


Figure S4. Related to Figure 3: (A-B) CFU count and OD₆₀₀ of *Lp*^{WCFS1} (turquoise) or *Lp*^{WCFS1} Δ *ldhDL* (light green) cultures at stationary phase in MRS (24h, A) or complete holidic diet (72h, B). Bars represent mean \pm SEM. We performed Mann-Whitney test to compare OD and CFU counts of *Lp*^{WCFS1} to *Lp*^{WCFS1} Δ *ldhDL*. (C) Growth rate of *Ap*^{WJL} on complete HD (black), *Lp*^{NC8} supernatant (green), *Lp*^{WCFS1} supernatant (turquoise) or *Lp*^{WCFS1} Δ *ldhDL* supernatant (light green). We performed Mann-Whitney test to compare the growth rate of *Ap*^{WJL} monoculture in HD to to the growth rate of *Ap*^{WJL} growing in the supernatant of interest. (D) *Ap*^{WJL} larval loads on complete HD (black) or complete HD supplemented with *Lp*^{NC8} supernatant (green), *Lp*^{WCFS1} supernatant (turquoise), *Lp*^{WCFS1} Δ *ldhDL* supernatant (light green) or DL-lactate at a final concentration of 0.6 g/L (red). We performed Kruskal-Wallis test followed by uncorrected Dunn's tests to compare each condition to the *Ap*^{WJL} condition (E) HPLC quantification of total amino acid concentration (μ M) in *Lp*^{NC8} supernatant during growth in liquid HD. Inner panel: *Lp*^{NC8} growth. Dot plots show mean and each point represent a biological replicate. We performed Kruskal-Wallis test followed by uncorrected Dunn's tests to compare each time point to T0. (F) Developmental timing of Germ Free (GF, light grey) larvae or GF larvae inoculated with 10⁵ CFU of *Ap*^{WJL} supplemented (black, grey filling) or not (black) with 300 μ L of sterile liquid HD. We performed Mann-Whitney test to compare the D₅₀ of *Ap*^{WJL} to *Ap*^{WJL} supplemented with steril HD. (G) Developmental timing of GF (grey) larvae or GF larvae supplemented with pure lactate (red), 300 μ L of sterile liquid HD (black) or 300 μ L of the different culture supernatants. ns: non-significant, *: p-value<0,05, **: p-value<0,005, ***: p-value<0,0005.

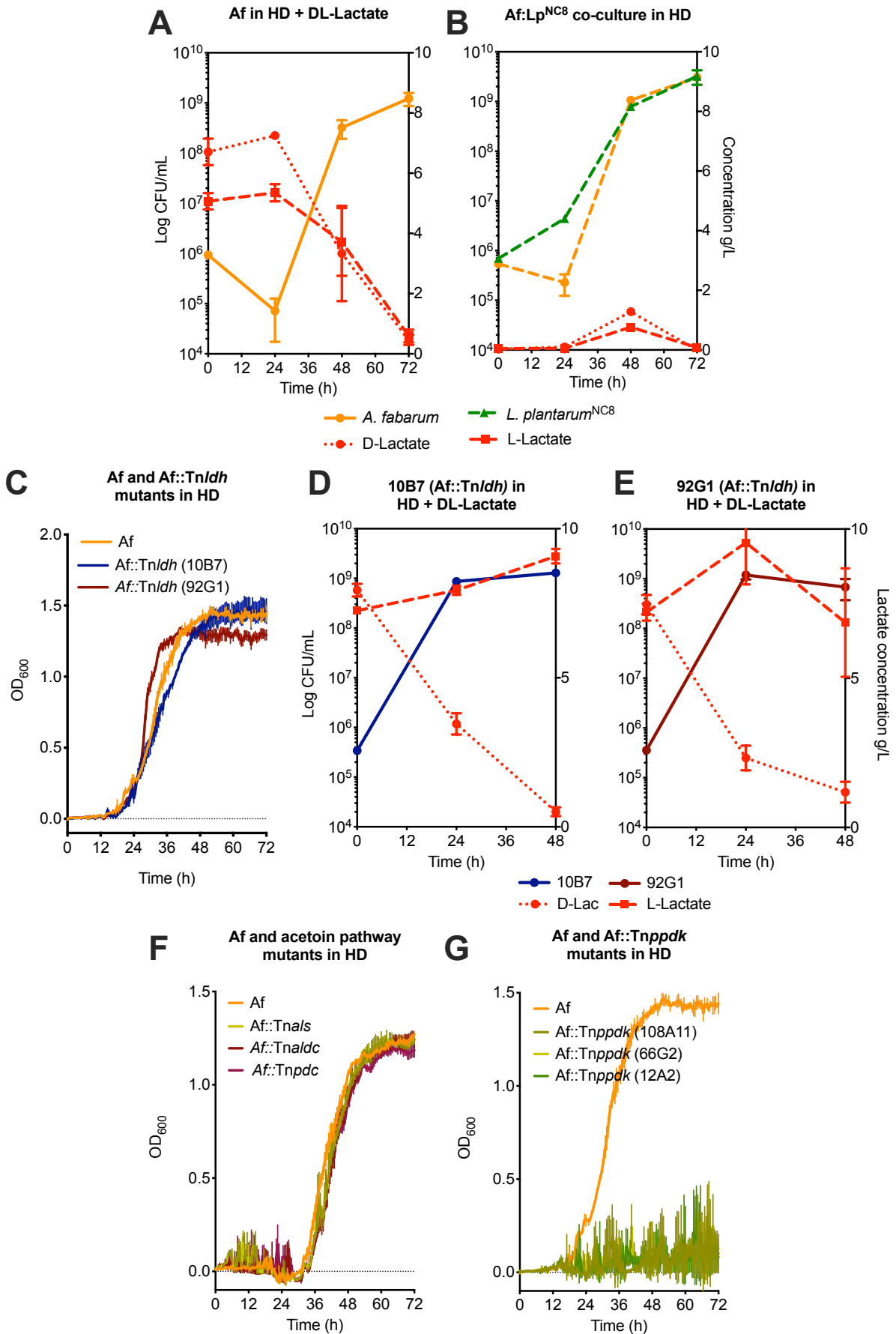


Figure S5. Related to Fig. 5: (A) Growth curve of *A. fabarum* (orange) in liquid HD

supplemented with DL-lactate. D- (dotted line) and L-lactate (dashed line) consumption (red) was quantified. (B) Growth curves in liquid HD of *Lp*^{NC8} (dashed green line) or *Af* (dashed orange line) in co-culture with the respective D- (dotted red line) or L-lactate (dashed red line) levels (red). (C) Growth curve of *A. fabarum* (orange), *Af::Tnldh* (10B7) (blue) or *Af::Tnldh* (92G1) (brown) in liquid HD. (D-E) Growth curves in liquid HD supplemented with DL-lactate of *Af::Tnldh* (10B7) (D) (blue line) or *Af::Tnldh* (92G1) (E) (brown line) with the respective D- (dotted red line) or L-lactate (dashed red line) levels (red). (F) Growth curves of *A. fabarum* (orange), *Af::Tnals* (light green), *Af::Tnaldc* (brown) or *Af::Tnfdc* (dark red) in liquid HD. (G) Growth curves of *A. fabarum* (orange), *Af::Tnppdk* (108A11) (green), *Af::Tnppdk* (66G2) (light green) or *Af::Tnppdk* (12A2) (dark green) in liquid HD. Symbols represent the means \pm SEM of three biological replicates.

SUPPLEMENTAL TABLES

Table S1: Final amino acid concentration supplemented to complete HD in the amino acid cocktail supplementation experiment. Related to Figure 4.

Amino acid	AA Mix (mg/L)		
	Ap @48h	Ap + Lactate @24h	Ap + Lactate @48h
Arg	-	36.802	1.337
His	7.467	39.088	12.911
Ile	-	14.913	-
Leu	9.091	19.230	-
Lys	-	71.720	33.243
Met	-	-	-
Phe	16.911	56.140	25.482
Thr	15.223	41.586	26.157
Val	5.115	22.169	17.314
Ala	-	21.621	80.409
Asp	0.241	13.920	-
Glu	4.703	-	-
Gly	-	8.284	-
Pro	-	-	-
Ser	18.407	38.394	-
Tyr	-	77.555	26.883
Total	77.160	461.428	223.740

Table S3. Strains used in this study. Related with Methods and all Figures.

Strain	Abbreviation	Genotype	Reference
<i>Acetobacter pomorum</i> ^{WJL}	Ap ^{WJL}	WT	Shin et al. 2011
<i>Lactobacillus plantarum</i> ^{NC8}	Lp ^{NC8}	WT	Axelsson L et al. 2012
<i>L. plantarum</i> ^{WCFS1}	Lp ^{WCFS1}	WT	Ferain et al. 1996
<i>L. plantarum</i> ^{WCFS1} Δ ldhDL	Lp ^{WCFS1} Δ ldhDL	Δ ldhDL	
<i>A. fabarum</i> ^{DsW_054}	Af	WT	Winans et al. 2017
<i>A. fabarum</i> ^{DsW_054} Tn:: <i>ldh</i> (10B7)	Af::Tn <i>ldh</i> (10B7)	Tn:: <i>ldh</i>	Winans et al. 2017 and Sommer & Newell 2018
<i>A. fabarum</i> ^{DsW_054} Tn:: <i>ldh</i> (92G1)	Af::Tn <i>ldh</i> (92G1)	Tn:: <i>ldh</i>	
<i>A. fabarum</i> ^{DsW_054} Tn:: <i>als</i>	Af::Tn <i>als</i>	Tn:: <i>als</i>	
<i>A. fabarum</i> ^{DsW_054} Tn:: <i>aldc</i>	Af::Tn <i>aldc</i>	Tn:: <i>aldc</i>	
<i>A. fabarum</i> ^{DsW_054} Tn:: <i>pdc</i>	Af::Tn <i>pdc</i>	Tn:: <i>pdc</i>	
<i>A. fabarum</i> ^{DsW_054} Tn:: <i>ppdk</i> (108A11)	Af::Tn <i>ppdk</i> (108A11)	Tn:: <i>ppdk</i>	
<i>A. fabarum</i> ^{DsW_054} Tn:: <i>ppdk</i> (66G2)	Af::Tn <i>ppdk</i> (66G2)	Tn:: <i>ppdk</i>	
<i>A. fabarum</i> ^{DsW_054} Tn:: <i>ppdk</i> (12A2)	Af::Tn <i>ppdk</i> (12A2)	Tn:: <i>ppdk</i>	

TRANSPARENT METHODS

***Drosophila* diets, stocks and breeding**

Drosophila stocks were reared as described previously (Erkosar et al., 2015). Briefly, flies were kept at 25°C with 12/12-hour dark/light cycles on a yeast/cornmeal medium containing 50 g/L of inactivated yeast, 80 g/L of cornmeal, 7.4 g/L of agar, 4 mL/L of propionic acid and 5.2 g/L of nipagin. Germ-free stocks were established as described previously (Erkosar et al., 2014) and maintained in yeast/cornmeal medium supplemented with an antibiotic cocktail composed of kanamycin (50 µg/mL), ampicillin (50 µg/mL), tetracycline (10 µg/mL) and erythromycin (5 µg/mL). Axenicity was tested by plating fly media on nutrient agar plates. *Drosophila yw* flies were used as the reference strain in this work.

Experiments were performed on Holidic Diet (HD) without preservatives. Complete HD, with a total of 8 g/L, 16 g/L or 20 g/L of amino acids, were prepared as described by Piper et al. using the fly's exome matched amino acid ratios (FLYAA) (Piper et al., 2017). Briefly, sucrose, agar, amino acids with low solubility (Ile, Leu and Tyr) as well as stock solutions of metal ions and cholesterol were combined in an autoclavable bottle with milli-Q water up to the desired volume, minus the volume of solutions to be added after autoclaving. After autoclaving at 120°C for 15 min, the solution was allowed to cool down at room temperature to ~60 °C. Acetic acid buffer and stock solutions for the essential and non-essential amino acids, vitamins, nucleic acids and lipids precursors were added. Single nutrient deficient HD (Fig. 2 and Fig. 3C) were prepared following the same recipe excluding the nutrient of interest (named HD Δ X, X being the nutrient omitted) as described in (Consuegra et al., 2020). Tubes used

to pour the HD were sterilized under UV for 20 min. HD was stored at 4°C until use, for no longer than one week.

Banana diet was prepared with 200 mL of mixed banana, 300 mL of water and 3.5 g of agar. After autoclaving at 120°C for 15 min, 10 mL of diet were poured into UV-sterilized tubes. Banana diet was stored at 4°C and used the next day.

Bacterial strains and growth conditions

Strains used in this study are listed in Table S3. *A. pomorum* was cultured in 10 mL of Mannitol Broth (Bacto peptone 3 g/L, yeast extract 5 g/L, D-mannitol 25 g/L) in 50 mL flask at 30°C under 180 rpm agitation during 24h. *A. fabarum* strains were cultured in 10 mL of YPD (yeast extract 10 g/L, Bacto peptone 10 g/L, Glucose 8 g/L) in 50 mL flask at 30°C under 180 rpm agitation during 24h. *L. plantarum* strains were cultured in 10 mL of MRS broth (Carl Roth, Germany) in 15 mL culture tubes at 37°C, without agitation, overnight. Liquid or solid cultures of Af::Tn were supplemented with kanamycin (Sigma-Aldrich, Germany) at a final concentration of 50 µg/mL. CFU counts were performed for all strains on MRS agar (Carl Roth, Germany). For selective isolation of *Acetobacter* or *Lactobacillus* during cocultures or bi-association, MRS plates were supplemented with ampiciline (10 µg/mL) or kanamycin (50 µg/mL), respectively. Appropriated dilutions were plated using the Easyspiral automatic plater (Intersciences, Saint Nom, France). The MRS agar plates were then incubated for 24-48h at 30°C for *Acetobacter* strains or 37°C for *Lactobacillus*. CFU counts were done using the automatic colony counter Scan1200 (Intersciences, Saint Nom, France) and its counting software.

Bacterial growth in liquid HD

To assess bacterial growth in the fly nutritional environment we used a recently developed liquid HD comprising all HD components except agar and cholesterol (Consuegra et al., 2020). Liquid HD was prepared as described for solid HD. Single nutrient deficient liquid HD was prepared following the same recipe excluding the nutrient of interest. After growth in rich media, the strain to be tested was washed with PBS twice and inoculated at a final concentration of $\sim 10^6$ CFU/mL. For cocultures, the strains were inoculated in a 1:1 ratio. For growth assessment in microplates, 200 μ L of media were inoculated in triplicate. Cultures were incubated in 96-well microtiter plates (Nunc™ Edge 2.0. Thermo Fisher Scientific) at 30°C for 72h. Growth was monitored using an SPECTROstar^{Nano} (BMG Labtech GmbH, Germany) by measuring the optical density at 600 nm (OD_{600}) every 30 minutes. For growth assessment in flasks, 10mL of complete or single nutrient deficient HD were inoculated in triplicate. Cultures were incubated in 50 mL flasks at 30°C under 180 rpm during 72h. Bacterial growth was assessed by plating appropriated dilutions of the cultures every 24h on MRS agar as described above. In figures representing growth in flasks the symbols represent the means with standard error based on three biological replicates. Growth rates were computed by calculating the slope of the curve during exponential growth using SPECTROstar^{Nano} custom analysis software, (BMG Labtech GmbH, Germany). We performed Mann-Whitney test to compare the growth rate among conditions.

Bacterial growth in solid HD

Bacterial CFUs in HD were assessed in microtubes containing 400 μ L of the diet of interest and 0.75–1 mm glass microbeads. Microtubes were inoculated with $\sim 10^4$ CFU of Ap^{WJL} or Lp^{NC8} or a $\sim 10^4$ CFU of a 1:1 mixture of Ap^{WJL} and Lp^{NC8} for coculture. To

assess grow with larvae, 5 first-instar larvae, were added. The tubes were incubated at 25°C. After incubation, 600µL of PBS were added directly into the microtubes. Samples were homogenized with the Precellys 24 tissue homogenizer (Bertin Technologies, Montigny-le-Bretonneux, France). Lysates were diluted in PBS and plated on MRS. CFU counts were assessed as described above.

Developmental timing determination

Axenic adults were placed in sterile breeding cages overnight to lay eggs on sterile HD. The HD used to collect embryos always matched the experimental condition. Fresh axenic embryos were collected the next morning and seeded by pools of 40 in tubes containing 10mL of the HD to test. Unless otherwise stated, in mono-associated conditions a total of $\sim 10^5$ CFU of the strain of interest, washed on PBS, was inoculated on the substrate and the eggs. For bi-association $\sim 10^5$ CFU of a 1:1 mixture of Ap^{WJL} and Lp^{NC8} were inoculated. For heat killed (HK) conditions, washed cells of Ap^{WJL} or Lp^{NC8} were incubated 3h at 65°C. Once at room temperature, embryos were inoculated with $\sim 10^5$ or $\sim 10^9$ CFU. In the germ-free conditions, bacterial suspensions were replaced with sterile PBS. When testing the effect of bacterial by-products on developmental timing, 300 µL of supernatants of a 72h culture on complete HD of the strain of interest was added to the GF or mono-associated embryos. For the lactate supplementation experiments, DL-lactate, D-lactate or L-lactate (Sigma-Aldrich, Germany) were added to a final concentration of 0.6 g/L on GF or mono-associated eggs. For the amino acid cocktail supplementation experiment (Fig. 4), solid complete HD was supplemented with a solution containing the amino acid mixes described in Table S1.

After inoculation, the tubes were incubated at 25°C with 12/12-hour dark/light cycles. The emergence of pupae was scored every day until all pupae had emerged. The experiment was stopped when no pupae emerged after 30 days. Each gnotobiotic or nutritional condition was inoculated in five replicates. D_{50} was determined using D50App (<http://paulinejoncour.shinyapps.io/D50App>) as described previously (Matos et al., 2017). D_{50} heatmap represent the average of the five replicates of each gnotobiotic and nutritional condition. Fig 2K was done using the `imagesc` function on MATLAB (version 2016b. MathWorks, Natick, Massachusetts). Developmental timings are represented as boxplots showing the minimum, maximum and median where each point is a biological replicate. We performed Kruskal-Wallis test followed by uncorrected Dunn's tests to compare each gnotobiotic condition to GF or the condition indicated on the figure.

Larval size measurements

Axenic adults were placed in sterile breeding cages overnight to lay eggs on sterile HD. Fresh axenic embryos were collected the next morning and seeded by pools of 40 in tubes containing 10mL of complete HD. For the mono-associated conditions a total of $\sim 10^5$ CFU Ap^{WJL} or Lp^{NC8}, washed on PBS, was inoculated on the substrate and the eggs. For biassociation $\sim 10^5$ CFU of a 1:1 mixture of Ap^{WJL} and Lp^{NC8} were inoculated. For the lactate supplementation experiments, DL-lactate was added to a final concentration of 0.6 g/L on Ap^{WJL} mono-associated eggs. After inoculation, the tubes were incubated at 25°C with 12/12-hour dark/light cycles until collection of larvae. *Drosophila* larvae were randomly collected every day until day seven after inoculation and processed as described previously (Erkosar, 2015). Larval longitudinal length of individual larvae was quantified using ImageJ software.

Microbial larval load in solid HD

Axenic adults were placed in sterile breeding cages overnight to lay eggs on sterile HD. Fresh axenic embryos were collected the next morning and seeded by pools of 40 in tubes containing 10mL of complete HD supplemented with 0.08% of erioglaucine disodium salt (Sigma-Aldrich, Germany). For the mono-associated conditions a total of $\sim 10^5$ CFU Ap^{WJL} or Lp^{NC8}, washed on PBS, were inoculated on the substrate and the eggs. For biassociation $\sim 10^5$ CFU of a 1:1 mixture of Ap^{WJL} and Lp^{NC8} were inoculated. When testing the effect of bacterial by-products on Ap^{WJL} larval load, 300 μ L of supernatants of a 72h culture on complete HD of the strain of interest was added to mono-associated embryos. After inoculation, the tubes were incubated at 25°C with 12/12-hour dark/light cycles until collection of larvae. *Drosophila* larvae were collected every day until five days after inoculation. We selected larvae with a blue gut to eliminate non-feeding individuals. Larvae were surface sterilize by rinsing once in ethanol 70% and twice in sterile PBS and placed in pools of 10 larvae/replicate/condition in 1.5 mL microtubes containing 500 μ L of sterile PBS and 0.75–1 mm glass microbeads. Samples were homogenized with the Precellys 24 tissue homogenizer (Bertin Technologies, Montigny-le-Bretonneux, France). Lysates dilutions (in PBS) were plated on MRS and CFU counts were assessed as described above. Microbial larval loads are represented as dot plots where each point represents a biological replicate comprising the average microbial load of a pool of 10 larvae. We performed Mann-Whitney test to compare microbial loads in mono-association to microbial loads in biassociation for the strain of interest at each time point.

DL-Lactate quantification

Mono-cultures of Ap^{WJL}, Lp^{NC8}, Lp^{WCFS1}, Lp^{WCFS1}ΔldhDL, Af and co-cultures of Ap^{WJL}:Lp^{NC8} and Af:Lp^{NC8} were grown in liquid complete HD as described above. Samples were taken at time 0h and every 24h for 72 h. After centrifugation (5000 rpm, 5 min) to remove cells, D and L lactate concentrations were measured in the supernatants using the D-Lactate and L-Lactate Assay Kit, respectively (Megazyme, Pontcharra-sur-Turdine, France), following the manufacturers' recommendations.

Amino acid quantification by HPLC

In order to quantify Arg, Ile and Leu production in depleted media (Fig. 2H-J), PBS washed Ap^{WJL}, Lp^{NC8} or Ap^{WJL}:Lp^{NC8} were grown in liquid HDΔArg, HDΔIle or HDΔLeu as described above. Samples were collected every 24h for 72h. CFU counts were assessed as described above and supernatants were stored at -20°C until use. To test total protein production by Lp^{NC8} (Fig. S4E) PBS washed Lp^{NC8} was grown in complete HD as described above. Supernatants were collected every 24h for 72h and stored at -20°C until use.

To test Ap^{WJL} amino acid production upon DL-lactate supplementation (Fig. 4A-B), PBS washed Ap^{WJL} was grown in complete HD supplemented or not with DL-lactate at final concentration of 20 g/L as described above. Supernatants were collected every 24h for 72h. CFU counts were assessed as described previously and supernatants were stored at -20°C until use.

Amino acid quantification was performed by HPLC from the supernatants. All proteinogenic amino acids were quantified except Cysteine, Tryptophan, Glutamine and Asparagine. Samples were crushed in 320 μl of ultra-pure water with a known quantity of norvaline used as the internal standard. Each sample was submitted to a

classical protein hydrolysis in sealed glass tubes with Teflon-lined screw caps (6N HCl, 115°C, during 22h). After air vacuum removal, tubes were purged with nitrogen. All samples were stored at -20°C, and then mixed with 50 µL of ultra-pure water for amino acids analyses. Amino acid analysis was performed by HPLC (Agilent 1100; Agilent Technologies, Massy, France) with a guard cartridge and a reverse phase C18 column (Zorbax Eclipse-AAA 3.5 µm, 150 × 4.6 mm, Agilent Technologies). Prior to injection, the sample was buffered with borate at pH 10.2, and primary or secondary amino acids were derivatized with ortho-phthalaldehyde (OPA) or 9-fluorenylmethyl chloroformate (FMOC), respectively. The derivatization process, at room temperature, was automated using the Agilent 1313A autosampler. Separation was carried out at 40°C, with a flow rate of 2 mL/min, using 40 mM NaH₂PO₄ (eluent A, pH 7.8, adjusted with NaOH) as the polar phase and an acetonitrile/methanol/water mixture (45/45/10, v/v/v) as the non-polar phase (eluent B). A gradient was applied during chromatography, starting with 20% of B and increasing to 80% at the end. Detection was performed by a fluorescence detector set at 340 and 450 nm of excitation and emission wavelengths, respectively (266/305 nm for proline). These conditions do not allow for the detection and quantification of cysteine and tryptophan, so only 18 amino acids were quantified. For this quantification, norvaline was used as the internal standard and the response factor of each amino acid was determined using a 250 pmol/µl standard mix of amino acids. The software used was the ChemStation for LC 3D Systems (Agilent Technologies).

Metabolite Profiling

Samples were prepared from tubes inoculated as a DT experiment (see above) comprising 5 biological replicates per condition. Conditions included GF, Af and Af::Tn*ldh* (10B7) inoculated at $\sim 10^5$ CFU on complete HD in presence or not of a pool of 40 GF-eggs. For the lactate supplemented conditions, L-lactate (Sigma-Aldrich, Germany) was added to a final concentration of 0.6 g/L on mono-inoculated tubes (Fig. 6A). Tubes were incubated at 25°C with 12/12-hour dark/light cycles during 3 days. After incubation, a sample of minimum 100 mg was taken from the tubes. In the conditions including embryos, larvae were completely removed. Samples were stored at -80°C before sending to Metabolon Inc. (www.metabolon.com). Samples were extracted and prepared for analysis by Metabolon using standard solvent extraction method. The extracted samples were analysed using UltraHigh Performance Liquid Chromatography coupled to Tandem Mass Spectrometry. 321 compounds were identified by comparison to library entries of purified standards or recurrent unknown entities. Following log transformation and imputation of missing values, if any, with the minimum observed value for each compound, Welch's two-sample *t*-test was used to identify biochemicals that differed significantly between experimental groups.

SUPPLEMENTAL REFERENCES

Consuegra, J., Grenier, T., Baa-Puyoulet, P., Rahioui, I., Akherraz, H., Gervais, H., Parisot, N., Silva, P. da, Charles, H., Calevro, F., et al. (2020). *Drosophila*-associated bacteria differentially shape the nutritional requirements of their host during juvenile growth. *Plos Biol* 18, e3000681.

Erkosar, B., Combe, B., Defaye, A., Bozonnet, N., Puthier, D., Royet, J., and Leulier, F. (2014). *Drosophila* microbiota modulates host metabolic gene expression via IMD/NF- κ B signaling. *PLoS ONE* 9, e94729.

Erkosar, B., Storelli, G., Mitchell, M., Bozonnet, L., Bozonnet, N., and Leulier, F. (2015). Pathogen virulence impedes mutualist-mediated enhancement of host juvenile growth via inhibition of protein digestion. *Cell Host Microbe* 18, 445–455.

Matos, R.C., Schwarzer, M., Gervais, H., Courtin, P., Joncour, P., Gillet, B., Ma, D., Bulteau, A.-L., Martino, M., Hughes, S., et al. (2017). D-alanine esterification of teichoic acids contributes to *Lactobacillus plantarum* mediated *Drosophila* growth promotion upon chronic undernutrition. *Nat. Microbiol.* 2, 1635–1647.

Piper, M.D.W., Soultoukis, G.A., Blanc, E., Mesaros, A., Herbert, S.L., Juricic, P., He, X., Atanassov, I., Salmonowicz, H., Yang, M., et al. (2017). Matching dietary amino acid balance to the *In Silico*-translated exome optimizes growth and reproduction without cost to lifespan. *Cell. Metab.* 25, 610–621.